

---

# Cathodic Protection Field Trials on Prestressed Concrete Components, Final Report

---

PUBLICATION NO. FHWA-RD-97-153

JANUARY 1998



U.S. Department of Transportation  
**Federal Highway Administration**

Research and Development  
Turner-Fairbank Highway Research Center  
6300 Georgetown Pike  
McLean, VA 22101-2296



## FOREWORD

This report documents a study to demonstrate the feasibility of using cathodic protection on concrete bridge structures containing prestressed steel. This final report describes the installation, start-up, and operation of five different cathodic protection systems on three structures in different climate zones. Following nearly 3 years of monitoring, the cathodic protection systems and bridge components were evaluated and tests were conducted to determine the effects on the bond between concrete and prestressing steel, and the structural properties of the prestressing steel. Analysis of the data indicated that the application of cathodic protection had no adverse effect on either the mechanical properties of the prestressing steel or bond between the concrete and prestressing steel.

This report will be of interest to bridge engineers and designers of prestressed concrete structures. The investigation will also be of interest to owners, inspectors, design firms, and construction contractors who are involved with the rehabilitation of prestressed concrete bridges.



Charles J. Nemmers, P.E.  
Director, Office of Engineering  
Research and Development

## NOTICE

This document is disseminated under the sponsorship of the Department of Transportation in the interest of information exchange. The United States Government assumes no liability for its contents or use thereof. This report does not constitute a standard, specification, or regulation.

The United States Government does not endorse products or manufacturers. Trade or manufacturers' names appear herein only because they are considered essential to the object of this document.

1. Report No. FHWA-RD-97-153	2. Government Accession No.	3. Recipient's Catalog No.	
4. Title and Subtitle CATHODIC PROTECTION FIELD TRIALS ON PRESTRESSED CONCRETE COMPONENTS, FINAL REPORT		5. Report Date January 1998	
		6. Performing Organization Code	
		8. Performing Organization Report No.	
7. Author(s) J. E. Bennett and T. J. Schue			
9. Performing Organization Name and Address ELTECH Research Corporation 625 East Street Fairport Harbor, OH 44077		10. Work Unit No. (TRAIS) 3D4b	
		11. Contract or Grant No. DTFH61-92-C-0003	
		13. Type of Report and Period Covered Final Report December 1991 - January 1997	
12. Sponsoring Agency Name and Address Office of Engineering R&D Federal Highway Administration, HNR-10 6300 Georgetown Pike McLean, VA 22101-2296			
		14. Sponsoring Agency Code	
15. Supplementary Notes Contracting Officer's Technical Representative (COTR): Y. P. Virmani, HNR-10			
16. Abstract <p>This is the final report in a study to demonstrate the feasibility of using cathodic protection (CP) on concrete bridge structures containing prestressed steel. The interim report, FHWA-RD-95-032, has more details on the installation of selected CP systems. Past laboratory and test yard studies had indicated that overprotection could result in the evolution of atomic hydrogen and the embrittlement of prestressing steel. Systems utilizing catalyzed titanium mesh, conductive rubber, and arc-sprayed zinc anodes were installed on prestressed pilings and girders of the Howard Frankland Bridge in Tampa, Florida; and systems using flame-sprayed zinc and conductive paint anodes were installed on the soffit of prestressed box beams of the Abbey Road and West 130<sup>th</sup> Street bridges near Cleveland, Ohio.</p> <p>For most of the components tested, CP was achieved safely and reliably without reaching conditions that could result in embrittlement of prestressed steel. Operation of these CP systems was best achieved in constant voltage mode which, in most cases, prevented hydrogen generation. Analyses of data indicated that the application of CP had no adverse effect on either the mechanical properties of the prestressing steel or the bond between the prestressed steel and concrete.</p> <p>Two of the zones tested on bridges in Ohio experienced very non-uniform current density due to leaky joints, which caused localized regions of low resistance. In these cases, it was impossible to achieve CP criteria at sites where resistance was high, while at the same time precluding hydrogen generation at sites where resistance was low. Such prestressed concrete structures with leaky joints are not good candidates for CP.</p> <p>Also, Devanathan-type hydrogen probes used in this study were not reliable indicators of hydrogen generation, and the conductive paint anode used on the West 130<sup>th</sup> Street Bridge developed extensive blistering as a result of sensitivity to moisture content and/or brief periods of high current.</p>			
17. Key Words  Corrosion, cathodic protection, anodes, bridges, prestressed concrete, concrete, hydrogen embrittlement, cathodic protection criteria.		18. Distribution Statement  No restrictions. This document is available to the public through the National Technical Information Service, Springfield, Virginia 22161.	
19. Security Classif. (of this report) Unclassified	20. Security Classif. (of this page) Unclassified	21. No. of Pages 74	22. Price

# SI\* (MODERN METRIC) CONVERSION FACTORS

## APPROXIMATE CONVERSIONS TO SI UNITS

## APPROXIMATE CONVERSIONS FROM SI UNITS

Symbol	When You Know	Multiply By	To Find	Symbol	Symbol	When You Know	Multiply By	To Find	Symbol
<b>LENGTH</b>					<b>LENGTH</b>				
in	inches	25.4	millimeters	mm	mm	millimeters	0.039	inches	in
ft	feet	0.305	meters	m	m	meters	3.28	feet	ft
yd	yards	0.914	meters	m	m	meters	1.09	yards	yd
mi	miles	1.61	kilometers	km	km	kilometers	0.621	miles	mi
<b>AREA</b>					<b>AREA</b>				
in <sup>2</sup>	square inches	645.2	square millimeters	mm <sup>2</sup>	mm <sup>2</sup>	square millimeters	0.0016	square inches	in <sup>2</sup>
ft <sup>2</sup>	square feet	0.093	square meters	m <sup>2</sup>	m <sup>2</sup>	square meters	10.764	square feet	ft <sup>2</sup>
yd <sup>2</sup>	square yards	0.836	square meters	m <sup>2</sup>	m <sup>2</sup>	square meters	1.195	square yards	yd <sup>2</sup>
ac	acres	0.405	hectares	ha	ha	hectares	2.47	acres	ac
mi <sup>2</sup>	square miles	2.59	square kilometers	km <sup>2</sup>	km <sup>2</sup>	square kilometers	0.386	square miles	mi <sup>2</sup>
<b>VOLUME</b>					<b>VOLUME</b>				
fl oz	fluid ounces	29.57	milliliters	mL	mL	milliliters	0.034	fluid ounces	fl oz
gal	gallons	3.785	liters	L	L	liters	0.264	gallons	gal
ft <sup>3</sup>	cubic feet	0.028	cubic meters	m <sup>3</sup>	m <sup>3</sup>	cubic meters	35.71	cubic feet	ft <sup>3</sup>
yd <sup>3</sup>	cubic yards	0.765	cubic meters	m <sup>3</sup>	m <sup>3</sup>	cubic meters	1.307	cubic yards	yd <sup>3</sup>
<b>MASS</b>					<b>MASS</b>				
oz	ounces	28.35	grams	g	g	grams	0.035	ounces	oz
lb	pounds	0.454	kilograms	kg	kg	kilograms	2.202	pounds	lb
T	short tons (2000 lb)	0.907	megagrams (or "metric ton")	Mg (or "t")	Mg (or "t")	megagrams (or "metric ton")	1.103	short tons (2000 lb)	T
<b>TEMPERATURE (exact)</b>					<b>TEMPERATURE (exact)</b>				
°F	Fahrenheit temperature	5(F-32)/9 or (F-32)/1.8	Celcius temperature	°C	°C	Celcius temperature	1.8C + 32	Fahrenheit temperature	°F
<b>ILLUMINATION</b>					<b>ILLUMINATION</b>				
fc	foot-candles	10.76	lux	lx	lx	lux	0.0929	foot-candles	fc
fl	foot-Lamberts	3.426	candela/m <sup>2</sup>	cd/m <sup>2</sup>	cd/m <sup>2</sup>	candela/m <sup>2</sup>	0.2919	foot-Lamberts	fl
<b>FORCE and PRESSURE or STRESS</b>					<b>FORCE and PRESSURE or STRESS</b>				
lbf	poundforce	4.45	newtons	N	N	newtons	0.225	poundforce	lbf
lbf/in <sup>2</sup>	poundforce per square inch	6.89	kilopascals	kPa	kPa	kilopascals	0.145	poundforce per square inch	lbf/in <sup>2</sup>

NOTE: Volumes greater than 1000 l shall be shown in m<sup>3</sup>.

\* SI is the symbol for the International System of Units. Appropriate rounding should be made to comply with Section 4 of ASTM E380.

## TABLE OF CONTENTS

<b>CHAPTER 1. INTRODUCTION</b> .....	1
<b>CHAPTER 2. BRIDGE AND CATHODIC PROTECTION SYSTEM SELECTION</b> .....	5
SOLICITATION AND SCREENING OF CANDIDATE STRUCTURES.....	5
DETAILED TESTING OF TOP CANDIDATE STRUCTURES.....	6
CATHODIC PROTECTION SYSTEM SELECTION.....	9
<b>CHAPTER 3. SYSTEM INSTALLATION AND START-UP</b> .....	11
<b>HOWARD FRANKLAND BRIDGE</b> .....	11
Metallized Zinc Anode System Installation.....	11
Fiberglass Jacket/Titanium Mesh Anode Installation.....	12
Conductive Rubber Anode System Installation.....	14
Rectifier, Remote Monitoring Unit, and Wiring Installation.....	17
Cathodic Protection System Start-Up .....	18
<b>ABBEY ROAD BRIDGE</b> .....	20
Metallized Zinc Anode System Installation.....	20
Rectifier, Remote Monitoring Unit, and Wiring Installation.....	23
Cathodic Protection System Start-Up .....	23
<b>WEST 130<sup>th</sup> STREET BRIDGE</b> .....	25
Conductive Coating Anode System Installation.....	25
Rectifier, Remote Monitoring Unit, and Wiring Installation.....	27
Cathodic Protection System Start-Up .....	27
<b>CHAPTER 4. LONG-TERM TESTING AND MONITORING</b> .....	31
<b>HOWARD FRANKLAND BRIDGE</b> .....	31
Metallized Zinc Anode System.....	31
Fiberglass Jacket/Titanium Mesh Anode System.....	32
Conductive Rubber Anode System.....	35
<b>ABBEY ROAD BRIDGE</b> .....	38
<b>WEST 130<sup>th</sup> STREET BRIDGE</b> .....	40
<b>EMBEDDED HYDROGEN PROBES</b> .....	45
<b>CHAPTER 5. POST-MONITORING ANALYSES OF CONCRETE AND STEEL</b> .....	47
ACQUISITION OF SPECIMENS .....	47
HYDROGEN CONTENT AND MECHANICAL PROPERTIES OF STEEL .....	48
Experimental Procedure .....	48
Abbey Road Bridge.....	49
Howard Frankland Bridge.....	50

**TABLE OF CONTENTS**  
**(continued)**

QUALITY OF BOND AND INTEGRITY OF CONCRETE .....	52
Experimental Procedure .....	52
Abbey Road Bridge .....	53
Howard Frankland Bridge .....	59
<b>CHAPTER 6. CONCLUSIONS AND RECOMMENDATIONS .....</b>	<b>65</b>
<b>REFERENCES .....</b>	<b>67</b>

## LIST OF FIGURES

<u>Figure No.</u>	<u>Page</u>
1. Howard Frankland Bridge—zinc beam zones section view .....	11
2. Completed zinc anode on bottom of girder.....	12
3. Howard Frankland Bridge—mesh pile jacket zone section view.....	13
4. Howard Frankland Bridge—integral mesh anode pile jacket half assembly .....	13
5. Pumping grout into installed pile jacket with horizontal bracing to prevent jacket deflection .....	14
6. Completed titanium mesh anode zone .....	15
7. Howard Frankland Bridge—conductive rubber pile zone section view .....	15
8. Howard Frankland Bridge—conductive rubber anode system and cross section .....	16
9. Installed conductive rubber anode .....	16
10. Coated wire and prestressing strand connections .....	17
11. Hydrogen probe and reference electrode in excavation on piling.....	18
12. Abbey Road Bridge—box beam section view .....	21
13. Finished grooves on each side of the joint between adjacent box beams .....	22
14. Flame spraying of zinc onto prepared surface .....	22
15. E-Log I of Abbey Road Bridge .....	24
16. West 130 <sup>th</sup> Street Bridge—box beam section view .....	26
17. Roller application of conductive coating with polyethylene-covered frame used to catch coating spills and drips.....	27
18. Current density versus time for metallized zinc anode system.....	31
19. Potential versus time for metallized zinc anode system .....	33
20. Voltage versus time for fiberglass jacket/titanium mesh anode system.....	33
21. Current versus time for fiberglass jacket/titanium mesh anode system.....	34
22. Steel potential versus time for fiberglass jacket/titanium mesh anode system.....	35
23. Voltage versus time for conductive rubber anode system .....	36
24. Current versus time for conductive rubber anode system.....	36
25. Steel potential versus time for conductive rubber anode system.....	37
26. Voltage versus time for West 130 <sup>th</sup> Street Bridge.....	43
27. Current versus time for West 130 <sup>th</sup> Street Bridge .....	44
28. Steel potential versus time for West 130 <sup>th</sup> Street Bridge .....	44
29. Core taken from Beam #6 of Abbey Road Bridge in as-received condition.....	54
30. Section views of core taken from Beam #9 of Abbey Road Bridge.....	55
31. Optical microscope view showing fracture of core from Beam #2 of Abbey Road Bridge .....	56
32. EDS spectrum and photograph (600X) of the steel/concrete interface in specimen from Beam #2.....	58
33. Optical microscope views of the Howard Frankland Bridge samples.....	60
34. Prestressing steel/concrete interface surfaces in Howard Frankland Bridge samples....	62
35. EDS spectrum and photograph (600X) of the prestressing steel/concrete interface surface in Howard Frankland Bridge sample.....	63

## LIST OF TABLES

<u>Table No.</u>		<u>Page</u>
1.	Data prior to start-up of Howard Frankland Bridge .....	19
2.	Data prior to start-up of Abbey Road Bridge.....	24
3.	Data prior to start-up of West 130 <sup>th</sup> Street Bridge .....	28
4.	Incremental start-up data for West 130 <sup>th</sup> Street Bridge .....	29
5.	Operating data for metallized zinc anode system .....	32
6.	Operating data for fiberglass jacket/titanium mesh anode system .....	34
7.	Operating data for conductive rubber anode system.....	37
8.	Steel potentials on conductive rubber anode pilings as a function of elevation .....	38
9.	Potential decay test at Abbey Road Bridge after 15 months of operation.....	39
10.	Summary of operating data from Abbey Road Bridge .....	40
11.	Potential decay test at West 130 <sup>th</sup> Street Bridge after 14 months of operation .....	42
12.	Summary of operating data from West 130 <sup>th</sup> Street Bridge.....	42
13.	Hydrogen content data from Abbey Road Bridge samples .....	50
14.	CERT results for Howard Frankland Bridge samples .....	51

## CHAPTER 1. INTRODUCTION

The objectives of this study were to install durable, cost-effective cathodic protection (CP) systems on prestressed concrete (PS/C) bridge components, to evaluate the effectiveness of the applied CP systems in combating corrosion, and to identify all limitations of the systems and potential risks to the structures.

The work plan called for the installation of CP systems on three structures in each of three different climate zones. The systems were monitored for about 3 years and evaluated for their effectiveness in this application. The long-term effectiveness of embedded reference electrodes and hydrogen probes were also studied during the monitoring phase of the contract. Methods of operation, appropriate for CP of PS/C components, were tested and evaluated. Near the conclusion of the study, extracted steel and concrete specimens were evaluated to determine whether operation of the CP systems resulted in loss of bond strength or hydrogen embrittlement of the steel.

Prior to this study, there had been a great deal of concern regarding the practice of using cathodic protection to mitigate corrosion in bridge components containing prestressed steel. This concern stems from the fact that high-strength prestressing steel is particularly susceptible to cracking due to hydrogen embrittlement. If a cathodic protection system is installed and operated in such a way that the magnitude of polarization is excessive, then atomic hydrogen may be generated at the surface of the steel and embrittlement may occur.

This possibility has been investigated by many authors in the past, and it has been confirmed that excessive polarization is likely to result in embrittlement of high-strength prestressing steel. The thermodynamic potential at which hydrogen is generated in concrete with pH 12.5 is -1.055 V versus copper/copper sulfate reference electrode (CSE) or -0.981 V versus saturated calomel reference electrode (SCE).<sup>(1)</sup> Under a recent Federal Highway Administration (FHWA) study, Wagner and coworkers found that hydrogen was generated at the surface of highly stressed steel members embedded in concrete at potential levels consistent with thermodynamic considerations.<sup>(2)</sup> That is, the potential at which hydrogen is generated can be predicted from the pH of the environment by using Pourbaix diagrams. Hydrogen flow from cement-coated steel at a pH of 12.4 was first detected at a potential of -0.974 V versus SCE. Hartt conducted constant extension rate and slow strain rate testing of prestressing strands, and concluded that embrittlement cracking did not occur at potentials less negative than -0.900 V versus SCE.<sup>(3)</sup> Hope and Poland reported the onset of hydrogen evolution at an apparent voltage of -0.940 V versus CSE, but this may have been the result of using an unfiltered power supply with peak voltage excursions up to -1.37 V versus CSE.<sup>(4)</sup>

Only rarely have authors suggested that operation at potentials at or less negative than -0.900 V versus SCE may result in hydrogen embrittlement of prestressing steel. In a recent paper, Hartt has reported a reduction in fracture load at potentials positive to -0.900 V versus SCE and at a pH of 12.5 for notched specimens of prestressed steel.<sup>(5)</sup> These results are unexpected since this potential is nearly 100 mV too positive to allow hydrogen evolution. No

satisfactory explanation has been proposed for this anomaly, but these results have led Hartt to suggest that -0.900 V versus SCE may not necessarily be an appropriate lower potential limit for cathodic protection of prestressing steel. Wagner and coauthors suggested that the IR-free potential of any prestressed steel member should not be permitted to become more negative than -0.800 V versus CSE (-0.726 V versus SCE).<sup>(2)</sup> This recommendation is based on the conclusion that lower pH values surrounding steel embedded in concrete are possible where carbonation has occurred, at cracks in concrete, and beneath corrosion products resulting from chloride ion penetration. Lower pH results in the possibility of embrittlement at less negative potentials than those required in concrete of normal alkalinity. But this rationale fails to account for the effects of cathodic current, which tend to raise the pH at all protected steel surfaces, primarily as a result of oxygen reduction. Mathematical modeling, conducted in a Strategic Highway Research Program (SHRP) study, demonstrated that even small cathodic protection currents will quickly raise pH at any active steel surface to values greater than a pH of 13.<sup>(6)</sup>

Based on the previous reported work and the technical considerations discussed above, it seems highly unlikely that significant hydrogen embrittlement will occur at steel potentials less negative than -0.900 V versus SCE. The significance of embrittlement at potentials more negative than the threshold for hydrogen evolution is more difficult to assess. Most authors have agreed that hydrogen embrittlement and brittle fracture are likely to occur if the thermodynamic potential for hydrogen evolution is exceeded.<sup>(2,3,4)</sup> Various conditions have been identified under which significant embrittlement of prestressing strands may not occur, regardless of potential. Hartt has reported that if the prestressing strand is smooth (i.e., unnotched, uncorroded), then the potential dependence of hydrogen embrittlement is modest, and the system would be a good candidate for cathodic protection.<sup>(7)</sup> In this case, smooth specimens at potentials more negative than -1.200 V versus SCE failed to experience significant loss of fracture load. This led Hartt to propose electrochemical proof testing (ECPT) as a means of qualifying a bridge member for cathodic protection. The proposed ECPT test involves the installation of a temporary impressed current system at a location of maximum corrosion damage and polarization of one or more tendons to a potential of at least -1.200 V versus SCE. The absence of failure within a predetermined time period (approximately 2 days) would qualify the structure for cathodic protection. Passing this test implies that excessive polarization will not cause failure due to embrittlement. ECPT has not been field-tested, so the procedures for detecting failure and the consequences of failure are not well defined.

Hartt has also suggested that the chromium content of steels may be used to qualify structures for cathodic protection.<sup>(8)</sup> In this work, Hartt found relatively low strength and ductility for steel specimens under CP which had relatively high chromium content (0.24 compared to 0.02 weight percent). However, a subsequent study, which also employed a 0.24 weight percent chromium microalloyed steel, failed to show any embrittlement<sup>(9)</sup>. In the same study, Hartt found that the loss of steel cross section due to corrosion may also be used to qualify a structure for CP. The data suggest that steel with less than 13 percent loss of cross section will not experience significant hydrogen embrittlement due to cathodic polarization, regardless of potential.

More recently, Enos and coworkers have detected small amounts of hydrogen permeation even at modest levels of cathodic protection current, such as  $3.3 \text{ mA/m}^2$  ( $0.31 \text{ mA/ft}^2$ ).<sup>(10)</sup> This effect was accentuated in the submerged and splash zones where the saturated pore structure within the concrete hindered oxygen diffusion. But the critical hydrogen concentration for embrittlement ( $2 \times 10^{-7} \text{ mole H/cm}^3$ ) was not exceeded at current densities as high as  $13.3 \text{ mA/m}^2$  ( $1.24 \text{ mA/ft}^2$ ).

Considering the work discussed above, the extent and significance of embrittlement that can occur at potentials beyond the threshold for hydrogen evolution cannot be easily predicted. But the possibility and significance of brittle fracture still require that cathodic protection systems be operated in such a manner as to prevent potentials that make possible the evolution of atomic hydrogen.

CP system control is clearly important to avoid conditions that may lead to hydrogen embrittlement of prestressed steel. The most logical approach is to control the steel potential to a predetermined value, thus precluding potentials beyond the threshold for hydrogen evolution. But studies in the 1980's by Stratfull, and by Schell and Manning, demonstrated that potential control was difficult to achieve and often resulted in excessive current.<sup>(11,12)</sup> A more recent study by Wagner and coworkers also indicated that control of a cathodic protection system to a preset potential is difficult, and possibly impractical.<sup>(2)</sup>

Two different methods of CP control have been proposed for the case where prestressed components are involved: constant current and constant voltage. Wagner and coworkers have recommended constant-current operation with a potential limit.<sup>(2)</sup> Hartt has concluded that constant-current CP systems may not be appropriate for prestressed steel concrete structures unless a current-off potential limitation corresponding to a threshold of  $-0.900 \text{ V}$  versus SCE is included.<sup>(5)</sup> But, as discussed above, the study by Wagner and coworkers also determined potential control to be impractical.

Bazzoni and Lazzari recommended a maximum operating voltage (constant voltage) technique.<sup>(13)</sup> The authors of this study developed a mathematical relationship, assuming a uniform anode potential and an overprotection parameter, which defines a safe operating voltage at which hydrogen evolution is impossible. A major assumption made in this treatment is that the anode potential is uniform and equal at all points in the cathodic protection system. While it is likely that this is a good assumption for highly catalytic anodes, such as mixed-metal-oxide-coated titanium, it may not be appropriate for other anode types.



## **CHAPTER 2. BRIDGE AND CATHODIC PROTECTION SYSTEM SELECTION**

### **SOLICITATION AND SCREENING OF CANDIDATE STRUCTURES**

Task A of this contract called for the selection of three bridges with prestressed steel. One bridge was to be selected in each of three climate zones—tropical marine, temperate marine, and temperate noncoastal. Each bridge was to have prestressed concrete members totaling at least 465 m<sup>2</sup> (5000 ft<sup>2</sup>) of surface area, with the total of all three bridges having at least 2090 m<sup>2</sup> (22,500 ft<sup>2</sup>). The presence of active corrosion on at least a portion of the prestressed steel was considered imperative. It was also considered important that the candidate structures have prestressed strand regions that could be destructively sampled without reducing the structural capacity of the members. Also considered, but of lesser importance, were the cooperation of State and local department of transportation (DOT) personnel, and accessibility of structures for testing and installation.

Fourteen bridges were initially selected for on-site screening. These included three bridges in tropical marine, six bridges in temperate marine, and five bridges in temperate noncoastal environments. The evaluation and selection of candidate bridges were carried out by Webster Engineering Associates, Inc., from December 1991 to September 1992. The following bridges were visited and evaluated as candidates. Test results are detailed in the Contract Interim Report (Report No. FHWA-RD-95-032).

1. Howard Frankland Bridge, Interstate 275 over Tampa Bay between St. Petersburg and Tampa, Florida. (Tropical Marine)
2. Interstate 10 bridge over Lake Pontchartrain, between New Orleans and Slidell, Louisiana. (Tropical Marine)
3. Ocean Drive Bridge over Cayo de Oso Bay at the west entrance to Corpus Christi Naval Air Station, Corpus Christi, Texas. (Tropical Marine)
4. Route 10 (business) bridge over Cypress Creek, County Isle of Wight, Smithfield Station, Virginia. (Temperate Marine)
5. Route 306 bridge over Rappahannock River, at Tappahannock, Essex County, Virginia. (Temperate Marine)
6. Richmond-San Raphael Bridge, Interstate 580 over San Pablo Strait, Richmond, California. (Temperate Marine)
7. Bridges at Devil's Elbow State Park, Oregon Coastal Highway (mile point 178.75), north of Florence, Oregon. (Temperate Marine)

8. Bridge over Youngs Bay, Oregon Coastal Highway (mile point 4.91), Astoria, Oregon. (Temperate Marine)
9. Columbia River Bridge, U.S. Highway 101, between Astoria, Oregon, and Point Ellice, Washington. (Temperate Marine)
10. Sandusky Bay Bridge, State Route 2, Bay View, Ohio. (Temperate Noncoastal)
11. State Route 718 bridge over Interstate 81, Harrisonburg, Virginia. (Temperate Noncoastal)
12. U.S. Route 224 bridge over the eastbound entrance to the Lorain Airdocks, Akron Municipal Airport, Akron, Ohio. (Temperate Noncoastal)
13. U.S. Route 224 bridge over South Arlington Road, Akron, Ohio. (Temperate Noncoastal)
14. Interstate 80 bridge over U.S. Route 15, Milton, Pennsylvania. (Temperate Noncoastal)

#### DETAILED TESTING OF TOP CANDIDATE STRUCTURES

Following the screening of the 14 candidate structures described above, 3 structures were selected for more detailed testing. These included the Howard Frankland Bridge in Tampa, Florida (tropical marine), the Richmond-San Raphael Bridge in Richmond, California (temperate marine), and the Sandusky Bay Bridge in Sandusky, Ohio (temperate noncoastal). It was assumed that these would be the structures selected for this study.

The work on the Howard Frankland Bridge in Tampa was given first priority, since this structure was identified as an excellent candidate, meeting all of the selection criteria. Plans and specifications were prepared, and bids were received on June 14, 1993. All bids received were well over the budget estimate used in the original proposal due to the complexity of the structure and the difficulty of working over tidewater far from shore. The Richmond-San Raphael Bridge was rejected for work because it would also be an expensive installation, and because it duplicated many elements of the Howard Frankland Bridge. The Sandusky Bay Bridge was rejected because of very difficult access problems and general lack of corrosion activity.

Additional screening was then conducted on several bridges in the Cleveland, Ohio, area and two prestressed box-beam structures were selected that met the acceptance criteria. The three candidate bridges which were then confirmed for work under this contract were the Howard Frankland Bridge in Tampa, Florida (tropical marine); the Abbey Road Bridge in Cuyahoga County, Ohio (temperate noncoastal); and the West 130<sup>th</sup> Street Bridge in Cuyahoga County, Ohio (temperate noncoastal). Testing of these structures is summarized below. More detailed results are given in the Contract Interim Report (Report No. FHWA-RD-95-032).

1. Howard Frankland Bridge, Interstate 275 over Tampa Bay between St. Petersburg and Tampa, Florida. (Tropical Marine)

The Howard Frankland Bridge is a 3.2-km- (2-mi-) long structure spanning Tampa Bay. It was constructed in 1959 with pretensioned/prestressed beams and prestressed square pilings. The prestressed piles are 60-cm- (24-in-) square members with eight piles per bent in the low portions of the bridge. The girders have pretensioned strands and draped post-tensioned strands in sheaths. The soffits of the girders are about 2.7 m (9 ft) above the water.

Chloride concentration in the pilings was exceptionally high, ranging from 1.24 percent total chloride [ $17 \text{ kg/m}^3$  ( $48.5 \text{ lb/yd}^3$ )] near the concrete surface to an average of 0.14 percent total chloride [ $1.9 \text{ kg/m}^3$  ( $5.4 \text{ lb/yd}^3$ )] at the depth of the steel, 60 to 64 mm (2 to 2.5 in). Chloride concentrations in the beams were moderate, but still exceeded corrosion threshold in most samples. Concrete resistivity on the piles ranged from 15.9 k $\Omega$ -cm at the high-tide elevation to 52 k $\Omega$ -cm at the top of the piles. Resistivity on the beams ranged randomly between 62.9 and 124.8 k $\Omega$ -cm. Concrete resistivity, although somewhat high for the beams, was considered acceptable for cathodic protection. Half-cell potential readings taken on the piles indicated the presence of very active corrosion at the time of the measurement, with readings ranging from -269 to -553 mV and averaging -433 mV versus CSE. Potential readings taken on the beams show a general lack of corrosion occurring at the time of measurement, but other observations confirmed the presence of corrosion activity. Numerous pilings had vertical cracks and delaminations as a result of corrosion of the reinforcing steel. Minimal delaminations were found on the beams. Some corrosion was present near the ends of the beams, but was not as active as that in the pilings. Other tests determined that the concrete was not carbonated.

2. Abbey Road Bridge over Baldwin Creek, Cuyahoga County, Ohio. (Temperate Noncoastal)

The Abbey Road Bridge was constructed in 1970 with noncomposite prestressed box sections and an asphaltic overlay. The deck cross section consists of eight 1.2-m- (4-ft-) wide and two 0.9-m- (3-ft-) wide prestressed box beams. The bridge is superelevated and slopes at a rate of 4.2 cm/m (0.5 in/ft). The average annual snowfall is 137 cm (54 in), and salting is heavy during winter months. Some of the joints between box beams are leaking, and the elevation has allowed saltwater to run along the underside of some of the beams.

Chloride ion content in the concrete was low to moderate, varying from below detection to 0.11 percent total chloride [ $1.5 \text{ kg/m}^3$  ( $4.2 \text{ lb/yd}^3$ )]; but it was clear that the beams were very nonhomogeneous with regard to chloride content and that active corrosion was taking place in portions of the structure. Resistance testing on this structure was conducted by pressing a mesh anode and a sponge

lightly soaked with solution containing a wetting agent against the concrete surface. Experience has shown that concrete having a resistance reading of less than 3000  $\Omega$  is acceptable for cathodic protection. Concrete resistance measured at 14 locations on each of the 5 beams ranged from 190 to 3000  $\Omega$ , and averaged 110  $\Omega$ . This test again showed the beams to be nonhomogeneous. A half-cell potential survey conducted on the soffit side of the beams showed that potentials varied widely from +43 to -625 mV versus CSE. Potential readings more negative than -350 mV, indicating active corrosion at the time of measurement, comprised 37 percent of the total readings. The most negative readings (most corrosive) were associated with leaking joints, and occurred on beams 2, 3, 5, 7, and 9. Despite the presence of very active corrosion, no delaminations or cracks were found on the prestressed box members.

3. West 130<sup>th</sup> Street Bridge over Baldwin Creek, Cuyahoga County, Ohio. (Temperate, Noncoastal)

The West 130<sup>th</sup> Street Bridge over Baldwin Creek was constructed in 1961 with noncomposite, prestressed box sections and an asphaltic overlay. The deck cross section consists of 15 1.2-m- (4-ft-) wide prestressed box beams. The average annual snowfall is 137 cm (54 in), and the bridge is heavily salted during winter months. Some of the joints between box beams showed signs of leaking, and several areas underneath the bridge were covered with salt deposits.

Chloride ion content in the samples was low to moderate, ranging from 0.07 percent total chloride [0.95 kg/m<sup>3</sup> (2.7 lb/yd<sup>3</sup>)] at a depth of 12 to 25 mm (0.5 to 1 in), to 0.02 percent total chloride [0.25 kg/m<sup>3</sup> (0.7 lb/yd<sup>3</sup>)] at the level of the prestressing strands. It was clear that chloride ion content in this structure was very nonhomogeneous. Resistance testing on this structure was also conducted by pressing a mesh anode and a sponge lightly soaked with solution containing a wetting agent against the concrete surface. Resistance measurements varied greatly, ranging from 1050 to 7700  $\Omega$ , illustrating the nonhomogeneous nature of the structure. Half-cell potentials taken on the soffit side of the beams varied widely from +88 to -481 mV versus CSE. Potential readings more negative than -350 mV, indicating active corrosion at the time of measurement, comprised 21 percent of the total readings. Of those beams tested, the most negative (most corrosive) readings were recorded on beams 2, 3, and 5. Despite the presence of very active corrosion, no delaminations or cracks were found on the prestressed box members.

## CATHODIC PROTECTION SYSTEM SELECTION

An independent consultant was retained to select the most appropriate cathodic protection systems for each of the bridge structures chosen. These are the consultant's recommendations, made after reviewing information available in the literature and on the candidate structures.

### 1. Interstate 275, Howard Frankland Bridge over Tampa Bay, Tampa, Florida.

Thermally sprayed zinc was selected for the prestressed beams. It was not clear from available information whether the zinc would supply enough current sacrificially to adequately protect the prestressing steel. It was therefore decided to install two zinc zones, one to operate in impressed current mode, and one to operate in sacrificial mode, but could be converted to impressed mode if polarization proved to be inadequate.

For the prestressed pilings, impressed current systems using titanium mesh anode and conductive rubber anode were selected. It was also suggested that bulk zinc anodes should be installed below water level to minimize current bleed to footings and pile portions below low tide.

### 2. Abbey Road Bridge over Baldwin Creek, Cuyahoga County, Ohio.

Thermally sprayed zinc was recommended for the underside of the Abbey Road Bridge. Conductive paint was not recommended for this structure, since it was felt that the superelevation would cause water to run on the underside of the beams and compromise the durability of that anode. Systems requiring shotcrete were not chosen for this structure since little mechanical interlock was available, and because shotcrete would need to be formed at every joint.

### 3. West 130<sup>th</sup> Street Bridge over Baldwin Creek, Cuyahoga County, Ohio.

Conductive paint anode was recommended for the underside of the West 130<sup>th</sup> Street Bridge. Again, systems requiring shotcrete were not chosen since little mechanical interlock was available, and because shotcrete would require forming at every joint.



## CHAPTER 3. SYSTEM INSTALLATION AND START-UP

### HOWARD FRANKLAND BRIDGE

#### Metallized Zinc Anode System Installation

It was decided to cathodically protect the 10 bottom prestressing strands of 20 girders in each of 2 zones as shown in figure 1. Zinc coating was not required on the upper portions of the girders due to a lack of corrosion activity in this area. The two zinc anode zones, also shown in figure 2, each had an area of 359 m<sup>2</sup> (3865 ft<sup>2</sup>), totaling 718 m<sup>2</sup> (7730 ft<sup>2</sup>) for both zones. A thickness of 0.25 to 0.38 mm (10 to 15 mil) of 99.9-percent pure zinc was specified. During quality control monitoring of the installation, zinc thicknesses were measured between 0.28 and 0.36 mm (11 and 14 mil).

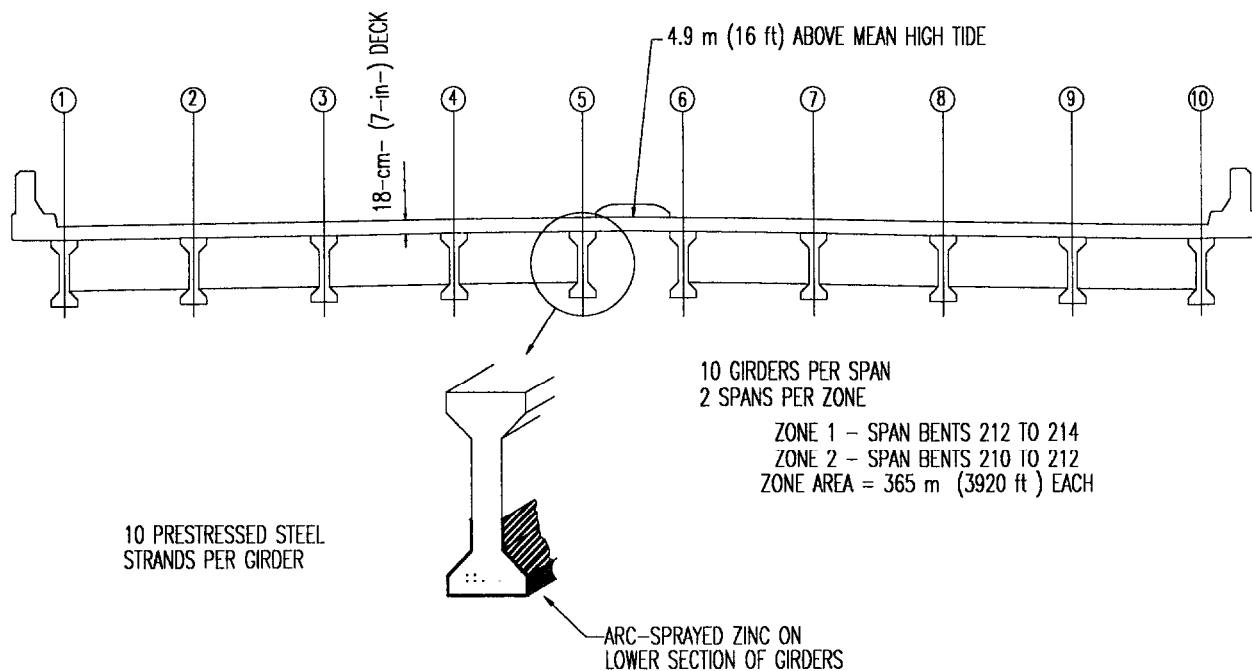


Figure 1. Howard Frankland Bridge—zinc beam zones section view.

Adhesion of the applied zinc coating was tested at one spot per girder using an Elcometer Adhesion Tester with a minimum specified pull-off strength of 690 kPa (100 lbf/in<sup>2</sup>). All 40 adhesion tests conducted were above the minimum strength and ranged from 690 to 2760 kPa (100 to 400 lbf/in<sup>2</sup>).

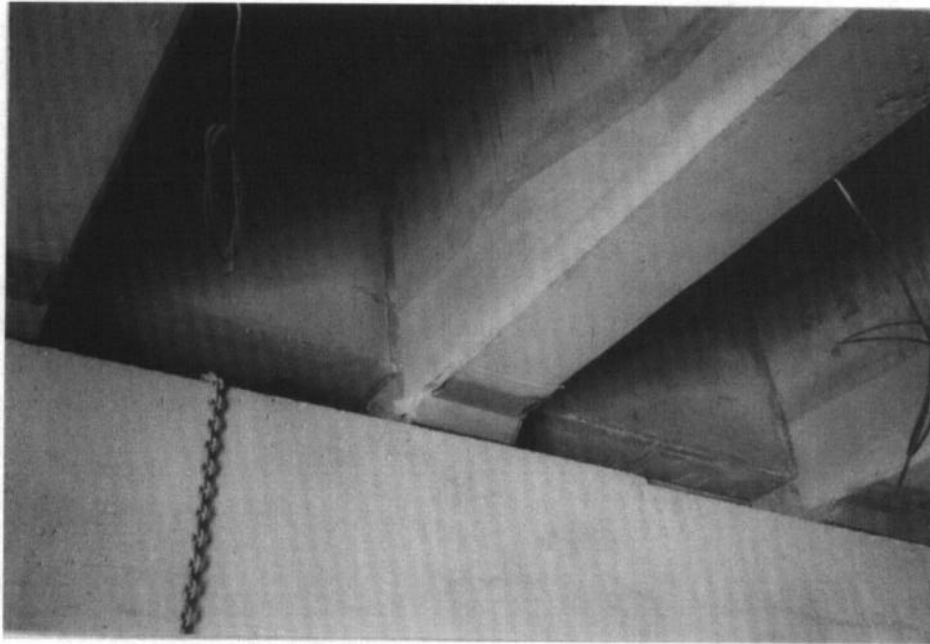


Figure 2. Completed zinc anode on bottom of girder.

#### Fiberglass Jacket/Titanium Mesh Anode System Installation

A fiberglass jacket/titanium mesh anode system zone was installed on the 60-cm- (24-in-) square prestressed piles of three bents, as shown in figure 3. The fiber-reinforced plastic (FRP) jacket consisted of two sections, each 1.22-m- (4-ft-) long with a male coupling on one side and a female coupling on the other side of the half-rectangle sections. When mated together, the two sections formed a rectangular jacket surrounding the pile with a 5.1-cm (2-in) annular space. The FRP jacket was fabricated to hold the activated titanium anode mesh and to retain the encapsulating concrete inside the jacket, as shown in figure 4.

After mounting the jackets to the pile, grout was pumped into the annular space between the jacket and the pile, as shown on figure 5.

- (1) Wooden forms were used to hold the jackets at the proper elevation. Five temporary aluminum frames were used to keep the jackets from expanding when being filled.
- (2) The jackets were filled in two stages. Each jacket was nearly half-filled, as shown in figure 5, while the exterior of the jacket was tapped with a hammer to remove air voids. After this procedure was completed on all the jackets, the second stage was pumped to fill each jacket. All the piles in one bent were filled at the same time.
- (3) After the jackets had been completely filled, additional grout was applied to the top of the jacket and beveled to slope downwards from the pile to the outside of the jacket.

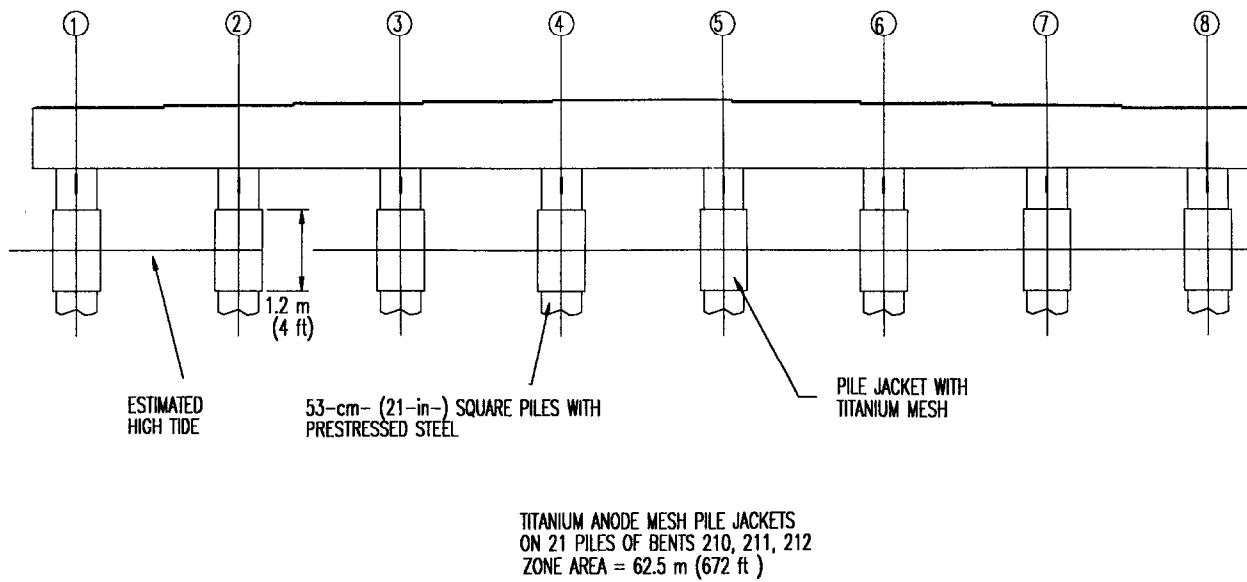


Figure 3. Howard Frankland Bridge—mesh pile jacket zone section view.

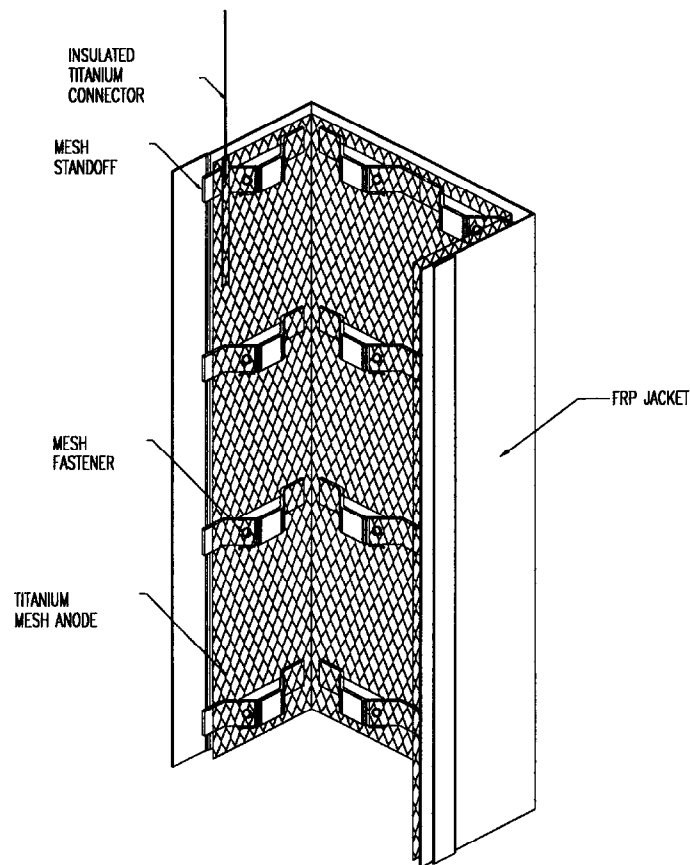


Figure 4. Howard Frankland Bridge—integral mesh anode pile jacket half assembly.



Figure 5. Pumping grout into installed pile jacket with horizontal bracing to prevent jacket deflection.

Care was taken to ensure that no air voids were present in the grout and that the grout completely encapsulated the titanium mesh. The finished pile jackets of the titanium mesh anode zone are shown on figure 6.

A layer of epoxy was then applied at the bottom of the jackets after the jackets were installed and the grout was cured. This layer covered a portion of the jacket, the exposed grout, and the adjacent pile area. The epoxy coating was applied to prevent leakage of cathodic protection current to seawater.

#### Conductive Rubber Anode System Installation

The conductive rubber anode system was installed on eight prestressed concrete piles as shown in figure 7. The anodes consisted of flat sheets of carbon-loaded ethylene propylene diene monomer (EPDM) conductive rubber. Anode sheets were held in place on the flat surfaces of the pile by four fiberglass panels, which also had a layer of nonconductive rubber adjacent to the fiberglass panels. One panel was mounted on each face of the pile. Five permanent stainless steel straps, which were wrapped around all four jacket segments, were used to press the jackets against the piles. Conductive rubber anode details are shown in figure 8.

The electrical connection to the titanium bar, which distributed current to the conductive rubber anode, was made with a butt splice. Connections were covered in nonconductive epoxy and heat-shrink tubing. A piling installed with conductive rubber anodes is shown in figure 9.

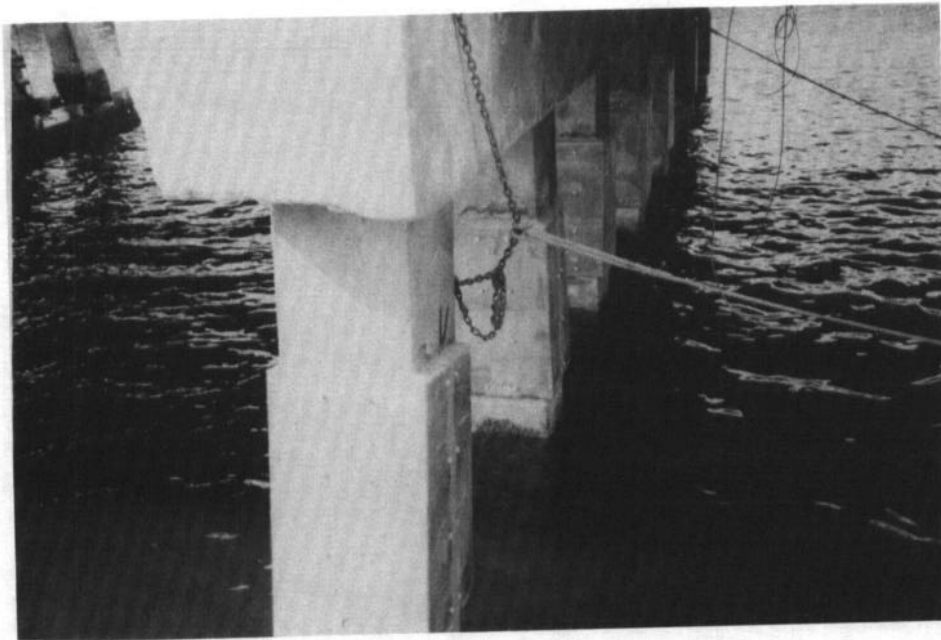


Figure 6. Completed titanium mesh anode zone.

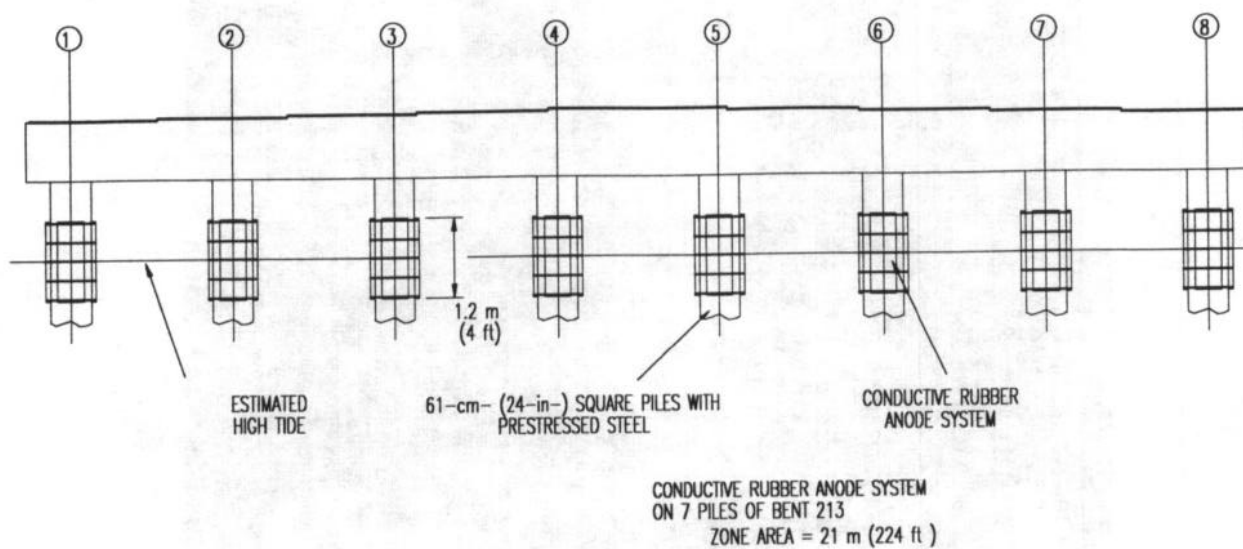


Figure 7. Howard Frankland Bridge—conductive rubber pile zone section view.

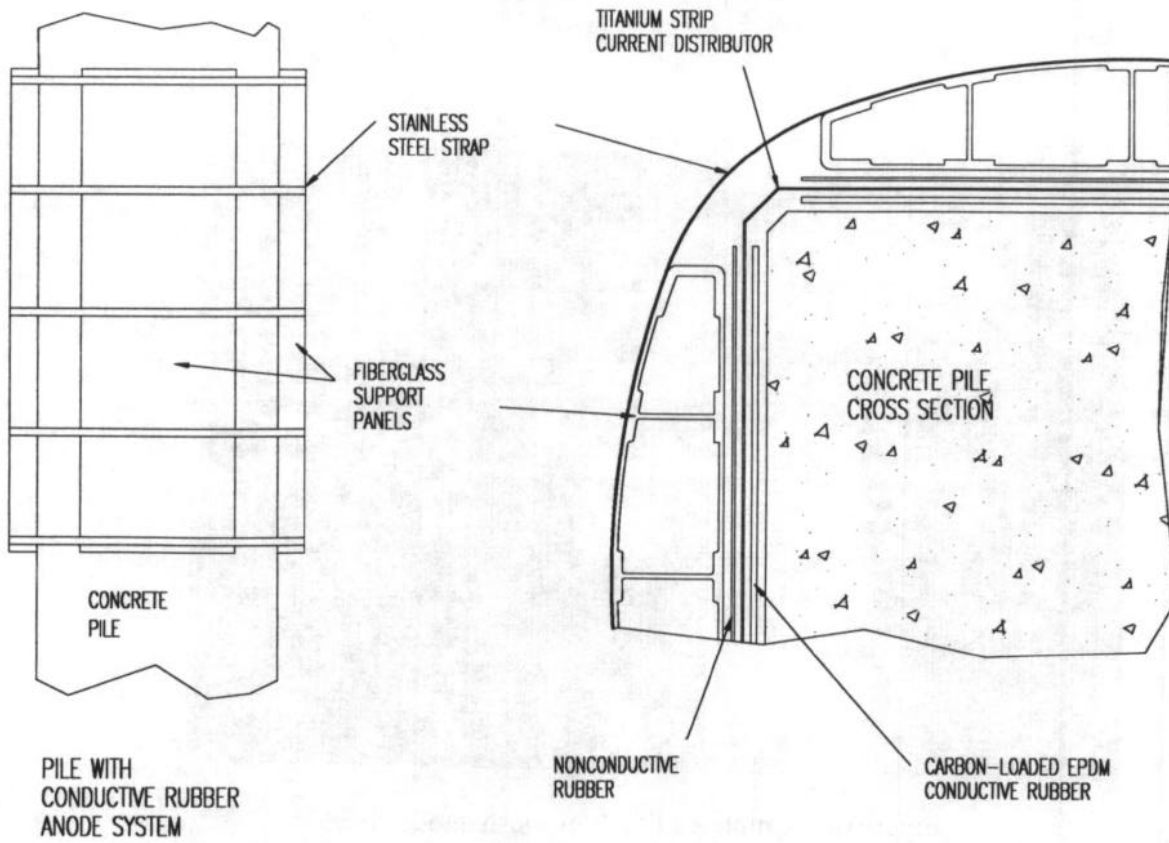


Figure 8. Howard Frankland Bridge—conductive rubber anode system and cross section.



Figure 9. Installed conductive rubber anode.

## Rectifier, Remote Monitoring Unit, and Wiring Installation

The power supply used on the Howard Frankland Bridge was designed with four circuits capable of independently controlling the four cathodic protection zones. Each circuit was capable of operating in either constant current or constant voltage mode, with a maximum current of 6 A and a maximum compliance voltage of 24 V.

A remote monitoring unit (RMU) was installed to remotely monitor the status of zone current, zone voltage, reference electrode voltage, and hydrogen cell readings for each anode zone. The system was designed to locally store, in battery-backed memory, 31 days of current, voltage, and potential readings on each cathodic protection zone. Since there were no phone lines on the bridge, a cellular phone was installed to access the RMU.

Electrical continuity of the prestressing strands was not assumed, and provisions were made to excavate the girders and pilings to assure full electrical continuity. Continuity was established by using stainless steel hose clamps and a 5.3-mm<sup>2</sup> (#10 AWG THHN) wire. These connections were then coated with nonconductive epoxy, as shown in figure 10, and excavations were filled with grout. This method was used for both system negative and reference ground connections, and provided good mechanical and electrical connection without damage to the strands.



Figure 10. Coated wire and prestressing strand connections.

Two silver/silver chloride reference electrodes were installed in each electrical zone. Each reference electrode was installed in an area of sound concrete where the most negative (corrosive) readings were recorded on the half-cell potential survey. The half-cell potential survey was conducted in accordance with ASTM C876-87. At each reference electrode site, a slot was excavated between reinforcing bars or prestressing strands without exposing the surrounding steel. The reference electrode was then installed in the slot and was backfilled with patching concrete with salt added to match the salt content of the surrounding concrete.

One embedded hydrogen cell was also installed in each electrical zone. The hydrogen cell was a sealed Devanathan probe with a palladium membrane capable of transmitting hydrogen. This membrane was connected to the system negative (steel), and if hydrogen was generated, the cell internally converted the flux of hydrogen into an electrical current. The current, if generated, is sensed as a millivolt signal and recorded by the RMU. The location and installation procedures for the hydrogen cell were similar to that used for the reference electrodes, except that backfill was made with salt-free patching concrete. A hydrogen probe and reference electrode are shown in an excavation in figure 11.



Figure 11. Hydrogen probe and reference electrode in excavation on piling.

#### Cathodic Protection System Start-Up

Data taken prior to start-up are presented in table 1. All reference-to-ground and anode-to-steel resistances were acceptable. Anode-to-steel and embedded reference cell-to-ground potentials were reasonable. Steel static potentials indicated little or no active corrosion on the beams (zones 1 and 2) at the time of measurement, and significant active corrosion

occurring on the piles (zones 3 and 4). The hydrogen probe readings showed an absence of hydrogen.

Table 1. Data prior to start-up of Howard Frankland Bridge.

<b>Area of Zones:</b>				
	Zone 1, arc-sprayed zinc beams = 364 m <sup>2</sup> (3920 ft <sup>2</sup> )			
	Zone 2, arc-sprayed zinc beams = 364 m <sup>2</sup> (3920 ft <sup>2</sup> )			
	Zone 3, titanium mesh grouted in pile jackets = 62.5 m <sup>2</sup> (672 ft <sup>2</sup> )			
	Zone 4, conductive rubber in pile jackets = 20.8 m <sup>2</sup> (224 ft <sup>2</sup> )			
<b>Anode-to-Steel Resistance:</b>		<b>Reference-to-Ground Resistance:</b>		
	Zone 1 = 0.52 ohms		R1-1 = 4400 ohms	
	Zone 2 = 0.68 ohms		R1-2 = 3000 ohms	
	Zone 3 = 0.37 ohms (new pile = 2.7)		R2-1 = 2200 ohms	
	Zone 4 = 2.4 ohms		R2-2 = 11 000 ohms	
<b>Potentials:</b>				
		<u>Ag/AgCl</u>	<u>Ag/AgCl</u>	
	<u>Anode-Steel</u>	<u>Reference 1</u>	<u>Reference 2</u>	<u>Hydrogen Cell</u>
Zone 1:	657 mV	-245 mV	-123 mV	0.0 mV
Zone 2:	662 mV	-208 mV	-187 mV	12.1 mV
Zone 3:	-625 mV	-557 mV	-378 mV	0.6 mV
Zone 4:	-547 mV	-316 mV	-530 mV	2.5 mV

(Note: Steel always connected to voltmeter positive.)

E-Log I tests were conducted on January 4 and 5, 1994, using the embedded Ag/AgCl reference electrodes, and using a saturated calomel reference electrode immersed in the seawater.

The current requirements for the arc-sprayed zinc zones 1 and 2, as determined from the E-Log I curves, were very low indicating little corrosion activity at the time of testing. Cathodic protection current ( $I_{CP}$ ) for zone 1 was established as 0.14 A, 0.39 mA/m<sup>2</sup> (0.036 mA/ft<sup>2</sup>), and protection current for zone 2 was established as 0.15 to 0.18 A, 0.41 to 0.49 mA/m<sup>2</sup> (0.038 to 0.046 mA/ft<sup>2</sup>).

The cathodic protection current requirement for the titanium mesh anode zone, as determined from the E-Log I curves, was 0.32 A, 5.16 mA/m<sup>2</sup> (0.48 mA/ft<sup>2</sup>).  $E_{CP}$  for the steel at this point was -640 mV. Given the corrosive state of the reinforcing steel in these piles, this seems to be a reasonable cathodic protection current. The cathodic protection potential does not risk hydrogen evolution. The E-Log I curve of the steel below water level, as monitored by the reference electrode in the seawater, showed only a slight response above 1.5 A. This demonstrated that a very small amount of current was leaking from zone 3 titanium mesh anodes into the seawater.

The E-Log I tests for the conductive rubber zone 4 were not very useful. No meaningful cathodic protection currents or potentials could be determined from the data. It appeared that the steel was not polarized 100 mV above static potentials until over 0.67 A, 32 mA/m<sup>2</sup> (3 mA/ft<sup>2</sup>) of current had been applied. Unlike the titanium mesh anode zone, the potential of the steel in the piles below water level did show a significant response above 0.50 A. At a current of 1.5 A or 72 mA/m<sup>2</sup> (6.7 mA/ft<sup>2</sup>), cathodic potentials of this steel exceeded -900 mV versus SCE. This shows a tendency for the conductive rubber anode to leak current to the portion of the piles beneath the seawater. This result was not unexpected, and it has been observed before by Florida DOT. It was expected that this tendency to leak current would decrease as the steel below water became polarized.

The response of the hydrogen cells was also monitored during start-up testing. For zones 1, 3, and 4, hydrogen cell response was minimal throughout the test. However, for the hydrogen cell in zone 2, a significant response was recorded at a current as low as 0.2 A, when steel potentials were only -223 and -97 mV versus Ag/AgCl. It appeared at that time that a response from this hydrogen cell was not a true indicator for atomic hydrogen generation. Shortly after start-up, other hydrogen cells also appeared to show false responses.

Based on start-up testing, it appeared that the zinc anodes in zones 1 and 2 could supply enough current in galvanic mode to protect the steel in the beams, and these zones were both activated without energizing the power supply.

Based on the E-Log I data, it was decided to start up zone 3 at about 0.35 A or 5.6 mA/m<sup>2</sup> (0.52 mA/ft<sup>2</sup>). This current was established at 1.4 V, and the zone was left in constant voltage mode at that voltage. Readings taken the next morning showed the IR-free potentials for zone 3 to be 110 and 132 mV more negative than their static potentials. Based on these readings, zone 3 was left in constant voltage control mode at 1.4 V.

The E-Log I data were of little help in establishing start-up conditions for zone 4. But since zone 4 current seemed to be easily polarizing steel below water level, more conservative control was used than for zone 3. Based mainly on previous Florida DOT experience, zone 4 was started up in constant voltage mode at 1.0 V. Readings taken the next morning showed IR-free potentials of steel in zone 4 to be almost the same as the original static potentials. This condition was due to early leakage of current to seawater, and polarization of steel adjacent to the anode was expected to increase with time.

## ABBEY ROAD BRIDGE

### Metallized Zinc Anode System Installation

A single metallized zinc anode zone was installed on the soffit of the bridge, which was comprised of 10 prestressed box beams totaling an area of 106 m<sup>2</sup> (1140 ft<sup>2</sup>). A layout and section view of the CP system are shown in figure 12.

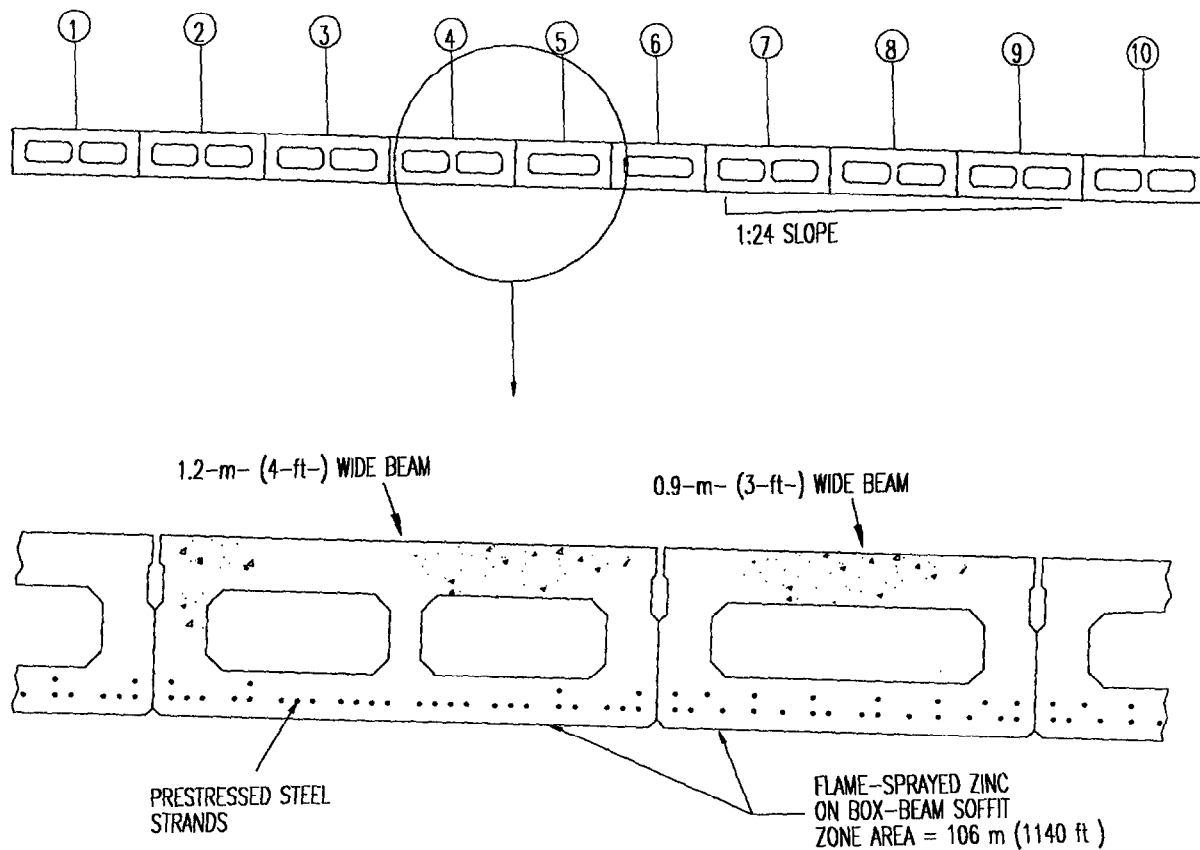


Figure 12. Abbey Road Bridge—box beam section view.

Several of the joints between the box beams were leaking, and because of the superelevation of the bridge, this caused water to run across the underside of the beams. This was a serious concern during installation since the concrete surface must be dry to ensure good bond of the zinc anode. A number of options were then tested to prevent the water from wetting the soffit side of the beams. The last option, sawcutting a drip edge, proved to be the most effective, and this is shown in figure 13. Once the sawcuts were completed, the soffit of the bridge could be dried with propane torches, and thermal spraying of the zinc anode proceeded without difficulty.

A zinc coating with a thickness of 0.25- to 0.38-mm (10- to 15-mil) was specified. Zinc was applied by flame spray, as shown on figure 14, and thickness ranged from 0.38 to 0.79 mm (15 to 31 mil).

Adhesion of the applied zinc coating was tested at one spot per box beam using an Elcometer Adhesion Tester. All 10 tests conducted were above the minimum bond strength of 690 kPa (100 lbf/in<sup>2</sup>), ranging from 1035 to 3280 kPa (150 to 475 lbf/in<sup>2</sup>).

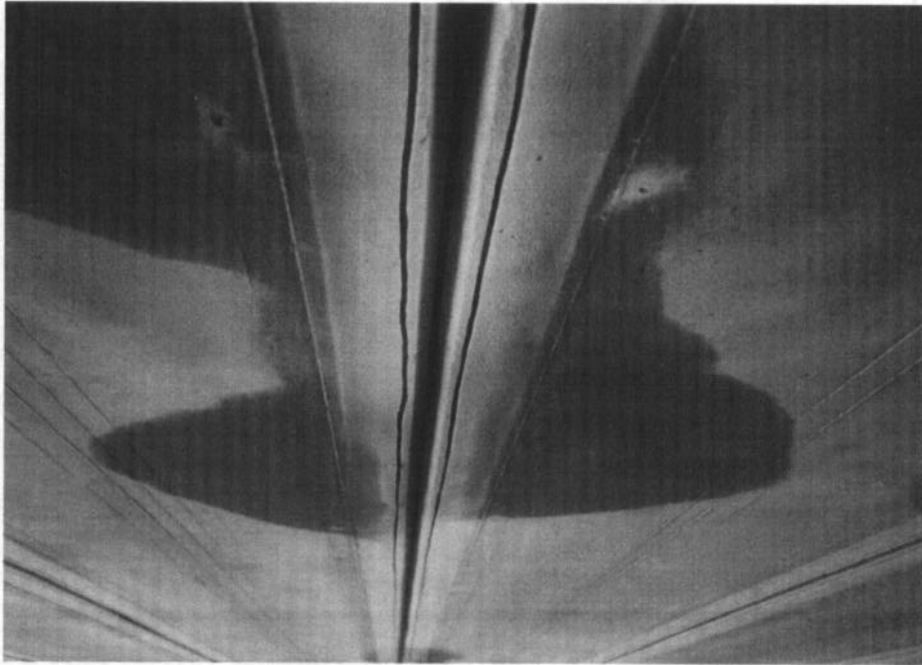


Figure 13. Finished grooves on each side of the joint between adjacent box beams.



Figure 14. Flame spraying of zinc onto prepared surface.

The zinc anode of each box beam was electrically isolated from the rest, so a single, continuous 1.3-cm- (0.5-in-) wide by 0.889-mm- (0.035-in-) thick titanium current distributor strip was held against the soffit with plastic anchors to electrically connect each box-beam anode. A layer of zinc was sprayed over the length of the conductor strip to achieve a more intimate contact. Although this method of contact looked adequate, testing revealed that several beam anodes remained electrically isolated. This was corrected at each beam by placing a nickel contact strip with multiple point contacts across the conductor strip and against the zinc anode. A titanium compression plate was placed over the nickel contact strip to ensure reliable connection.

### Rectifier, Remote Monitoring Unit, and Wiring Installation

The power supply was designed for operation in either constant-current or constant-voltage mode, with a maximum current of 6 A and a maximum compliance voltage of 24 V. As with the Howard Frankland Bridge, an RMU was installed to remotely monitor the status of the zone current, zone voltage, reference electrode voltage, and hydrogen cell readings. The system was designed to locally store, in battery-backed memory, 31 days of current, voltage, and potential readings.

All prestressed strands were discontinuous. The upper row of strands in each beam was not bonded to the lower row since chloride levels at the upper strands were too low to induce corrosion. Excavations for continuity bonding were made across the bottom of the beams to expose the bottom row of prestressing strands. The method of making connections to the prestressing strands for both the system negative and reference ground connections was then accomplished in the same manner as on the Howard Frankland Bridge trial in Florida. Continuity was established with stainless steel hose clamps and an insulated, 5.3-mm<sup>2</sup> (#10 AWG) copper wire, which was placed in each excavation. The connection was then coated with liquid plastic, and the excavations were filled with grout.

As with the Howard Frankland Bridge in Florida, two silver/silver chloride reference electrodes and one Devanathan hydrogen cell were installed in the most negative (corrosive) locations in the zone. The procedures for installation of reference electrodes and hydrogen cell were also the same as previously reported.

### Cathodic Protection System Start-Up

Data taken prior to start-up are presented in table 2. In addition to the embedded Ag/AgCl reference cells, potential wells were installed in two beams near leaking joints. This was done to enable potential measurement of steel in wet areas where current density is likely to be highest. The potential well in beam 4 is labeled "W-Well," and the one in beam 9 is labeled "E-Well." All potentials recorded at the potential wells, as well as potentials taken from the concrete surface, were taken using a portable saturated calomel reference electrode. All anode-to-steel and embedded reference-to-ground resistances were considered acceptable, although the reference-to-ground resistance for RC-2 was higher than normal. This was not

expected to have an impact on the results or conclusions of the test. Static potentials indicated that active corrosion was occurring at the steel at the time of the measurement.

Table 2. Data prior to start-up of Abbey Road Bridge.

---

Area of Zone: 106 m<sup>2</sup> (1140 ft<sup>2</sup>)

<p>Anode-to-Steel Resistance: 0.26 ohms</p>	<p>Reference-to-Ground Resistance: RC-1 = 2000 ohms RC-2 = 15 000 ohms</p>
---	--

Potentials:

RC-1	= -270 mV vs. Ag/AgCl (-364 mV vs. CSE)
RC-2	= -273 mV vs. Ag/AgCl (-367 mV vs. CSE)
W-Well	= -370 mV vs. SCE (-444 mV vs. CSE)
E-Well	= -582 mV vs. SCE (-656 mV vs. CSE)

---

E-Log I tests were conducted on April 26, 1994, using the embedded Ag/AgCl reference electrodes and portable saturated calomel reference electrodes in the potential wells. All four E-Log I curves, shown in figure 14, exhibit a straight-line portion. The cathodic protection current ranged from 1.15 to 1.50 A or 10.8 to 14.0 mA/m<sup>2</sup> (1.00 to 1.30 mA/ft<sup>2</sup>). This was considered reasonable for this structure. Cathodic protection potentials ranged from -380 to -830 mV versus Ag/AgCl (-474 to -904 mV versus CSE), indicating the nonhomogeneous nature of this structure.

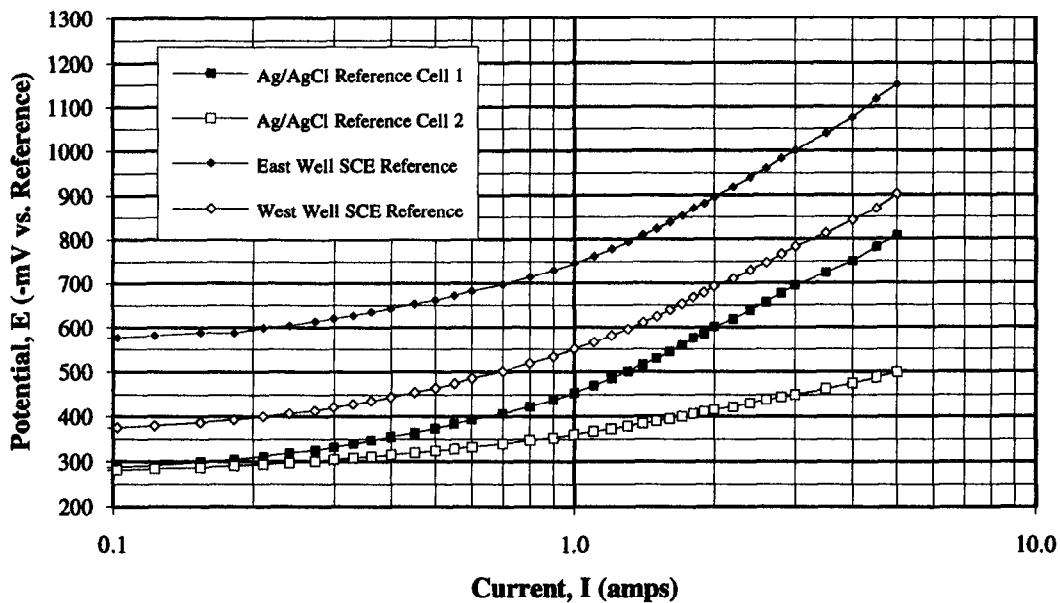


Figure 15. E-Log I of Abbey Road Bridge.

The data taken from the hydrogen cell were erratic, showing significant values at potentials too positive to result in generation of atomic hydrogen. This is the same result noted during start-up testing of systems on the Howard Frankland Bridge in Tampa, Florida. There was no obvious explanation for the apparent failure of the hydrogen cells in these systems.

Since the structure was subject to uneven wetting because of leaking joints between the box beams, there was concern that impressed current could lead to high localized current, which might result in potentials sufficiently negative to generate hydrogen at the prestressing steel. For this reason, it was decided to energize this system in sacrificial mode. It was felt that operation in sacrificial mode would limit the potentials on the protected prestressing steel and minimize the concern for hydrogen embrittlement.

Depolarization testing of the system on Abbey Road Bridge was conducted after 3 days of operation in sacrificial mode. Testing was conducted at the two embedded reference electrodes, the two potential wells, and at windows in the zinc anode at the south end of each beam. Current-on and current-off potentials were first taken at each location.

Final values for the 4-h depolarization were greater than 100 mV at all 14 test points, and average depolarization was 162 mV. Based on the 100-mV National Association of Corrosion Engineers (NACE) criterion as stated in Standard Recommended Practice RP0290-90, the steel was being adequately protected at the time of this test.

## **WEST 130<sup>th</sup> STREET BRIDGE**

### **Conductive Coating Anode System Installation**

The single conductive paint anode system zone was installed on the soffit of the bridge, which was comprised of 15 prestressed box beams totaling 223 m<sup>2</sup> (2400 ft<sup>2</sup>), as shown in figure 16.

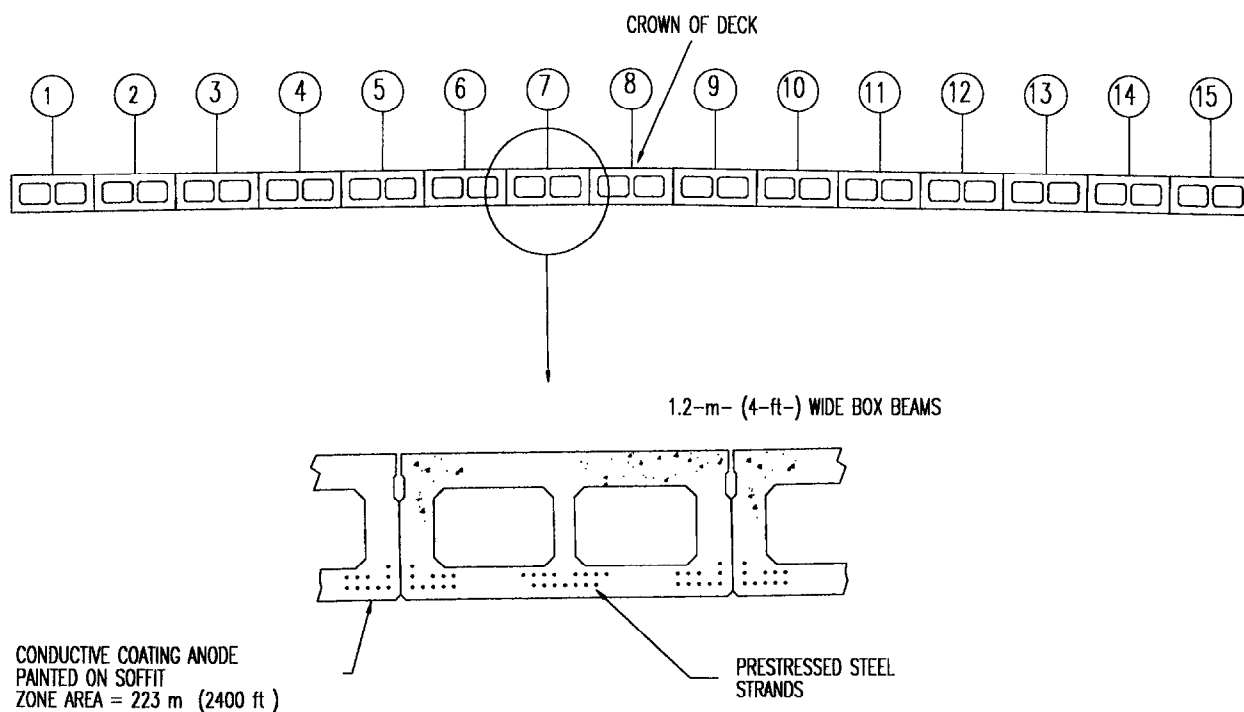


Figure 16. West 130<sup>th</sup> Street Bridge—box beam section view.

The single CP zone was instrumented with two Ag/AgCl reference electrodes, one in beam 2 and one in beam 15. One hydrogen probe was placed in beam 15, which had the most corrosive half-cell potential readings.

As with the Abbey Road Bridge, leaking of water through joints between the box beams presented a major problem. The manufacturer of the conductive coating indicated that the coating could be successfully applied only if the soffit was dry prior to and during the coating application and curing. The soffit was therefore prepared with sawcut drip edges as described for the Abbey Road Bridge, and installation of the coating was delayed until favorable weather resulted in a dry concrete surface during coating application and curing.

The conductive coating selected was Permarock SC5, a solvent-based coating with a successful record of field installations, particularly in Europe. This paint formulation is based on inert chlorinated polymers with a carbon matrix, which makes it very resistant to both acidic and alkali environments. When fully cured, its electrical resistance is less than 40  $\Omega$ /square when applied to a thickness of 150  $\mu\text{m}$  (6 mil).

Two coats of conductive coating were applied using rollers over an adhesion-promoting primer. A moveable, plastic-covered wooden frame (shown in figure 17) was placed on the ground under an area being painted to prevent drips and spills from entering Baldwin Creek. The coating thickness was measured during placement with a thickness gauge and after final application with a Tooke gauge. The specified minimum 0.25-mm (10-mil) dry-film thickness was achieved.

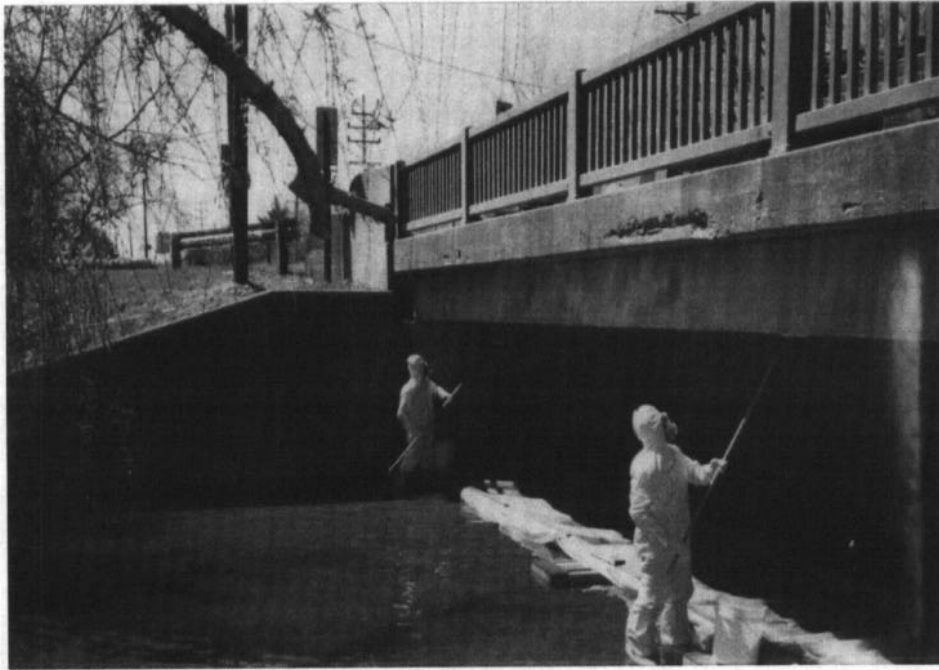


Figure 17. Roller application of conductive coating with polyethylene-covered frame used to catch coating spills and drips.

#### Rectifier, Remote Monitoring Unit, and Wiring Installation

The same power supply and remote monitoring unit were used for the West 130<sup>th</sup> Street Bridge as were used for the other bridges in this contract. As with the Abbey Road Bridge site, a telephone line was conveniently available and was used to access the RMU.

Again, all prestressed strands were discontinuous. The procedures used at the Abbey Road installation for continuity bonding, as well as for system negative and reference ground connections, were also used at this installation. All excavations were then filled with grout.

Placement and system wiring for system negatives, reference electrodes, and hydrogen cells were done in the same manner as at the Abbey Road installation.

#### Cathodic Protection System Start-Up

Data taken prior to start-up are presented in table 3. In addition to the embedded Ag/AgCl chloride reference cells, potential wells were installed in two beams at areas of significant wetness where current density is likely to be highest. The potential well in beam 2 is labeled "2W" and located near a scupper. The well in beam 12 is labeled "12W" and is located at the center feed wire.

Two more potential wells were installed in dry areas of beam 11, one (labeled "11N") near the center feed wire, and one (labeled "11F") far from the center feed wire, where voltage drop through the anode is greatest. All potentials recorded at the potential wells, as well as potentials taken from the concrete surface, were taken using a portable saturated calomel reference electrode. All anode-to-steel and embedded reference-to-ground resistances were acceptable. The static potentials taken with the embedded reference cells and the concrete surface in wet areas indicated that active corrosion was occurring at the time of the measurement.

Table 3. Data prior to start-up of West 130<sup>th</sup> Street Bridge.

---

Area of Zone:	
223 m <sup>2</sup> (2400 ft <sup>2</sup> )	
Anode-to-Steel Resistance:	Reference-to-Ground Resistance:
0.57 ohms	RC-1 = 3700 ohms
	RC-2 = 3100 ohms
Potentials:	
RC-1 = -371 mV vs. Ag/AgCl (-465 mV vs. CSE)	
RC-2 = -356 mV vs. Ag/AgCl (-450 mV vs. CSE)	
11N = -146 mV vs. SCE (-220 mV vs. CSE)	
11F = -114 mV vs. SCE (-188 mV vs. CSE)	
12W = -244 mV vs. SCE (-318 mV vs. CSE)	
2W = -330 mV vs. SCE (-404 mV vs. CSE)	

---

The manufacturer's recommendations state that the current is to be gradually increased to the desired current over several weeks of time. It was also considered possible that the high currents needed for E-Log I testing could damage the anode. The desired current was therefore determined by monitoring reference cell potentials and confirming sufficient polarization with polarization decay test results.

Since the box beams contained prestressed steel, it was essential to control corrosion with sufficient cathodic polarization of the steel and at the same time preclude evolution of atomic hydrogen and hydrogen embrittlement. The embedded silver/silver chloride reference cells were monitored during the current increase procedure to preclude operation at potentials sufficiently negative to permit hydrogen generation.

The system was energized in constant current mode at 0.48 A or 2.15 mA/m<sup>2</sup> (0.2 mA/ft<sup>2</sup>) on May 26, 1994. After 13 days, on June 8, 1994, the system current was increased to 0.96 A or 4.3 mA/m<sup>2</sup> (0.4 mA/ft<sup>2</sup>). On June 15, 1994, the system current was again increased to 1.44 A or 6.45 mA/m<sup>2</sup> (0.6 mA/ft<sup>2</sup>). The operating data at these current densities are shown in table 4.

Table 4. Incremental start-up data for West 130<sup>th</sup> Street Bridge.

	2.15 mA/m <sup>2</sup> (0.2 mA/ft <sup>2</sup> )	4.3 mA/m <sup>2</sup> (0.4 mA/ft <sup>2</sup> )	6.45 mA/m <sup>2</sup> (0.6 mA/ft <sup>2</sup> )
System Voltage (V)	1.66	2.05	2.30
Current (A)	0.48	0.96	1.44
Hydrogen Cell (mV)	1.7	0.0	0.0
Potential RC-1 (on) mV vs. Ag/AgCl	-594	-721	-840
Potential RC-2 (on) mV vs. Ag/AgCl	-600	-778	-930

Depolarization testing of the system on the West 130<sup>th</sup> Street Bridge was then conducted on August 4, 1994. Testing was conducted at the two embedded reference electrodes, four potential wells, and at windows in the conductive paint anode at the south of each beam. Final values for the 4-h depolarization were greater than 100 mV at all 21 test points. The average depolarization was 742 mV. Based on the 100-mV National Association of Corrosion Engineers (NACE) criterion as stated in Standard Recommended Practice RP0290-90, the steel was being adequately protected at the time of this test. However, several IR-free, instant-off potentials were sufficiently negative to suggest hydrogen was being generated at a current density of only 6.45 mA/m<sup>2</sup> (0.6 mA/ft<sup>2</sup>).

The system current density was then adjusted down to 3.2 mA/m<sup>2</sup> (0.3 mA/ft<sup>2</sup>) to allow for steel protection without reaching the hydrogen evolution potential.



## CHAPTER 4. LONG-TERM TESTING AND MONITORING

### HOWARD FRANKLAND BRIDGE

#### Metallized Zinc Anode System

Corrosion activity within the two zones with metallized zinc anodes was very localized, being limited mainly to the ends of the girders. Because of this, initial current requirements for these two zones were very low, and the zones were both started up in galvanic mode. It was expected that galvanic current would decrease with time, and that the power supplies would eventually need to be activated, thus converting from galvanic to impressed current mode of operation.

Current did decrease with time for the zinc in galvanic mode, as expected. This decrease is shown graphically on figure 18. Over the first 38 months of operation, current density decreased from  $1.6 \text{ mA/m}^2$  ( $0.15 \text{ mA/ft}^2$ ) to  $0.2 \text{ mA/m}^2$  ( $0.02 \text{ mA/ft}^2$ ). But throughout this period of time, adequate depolarization was recorded for the steel in these zones and the accepted polarization criterion of 100 mV was met. These data are shown in table 5. It is somewhat surprising that polarizations of over 200 mV were consistently achieved at such low current densities. This is due to the passive nature of most of the steel in these zones. Both of the zones with metallized zinc anodes were left in galvanic mode of operation following the monitoring phase of this contract.

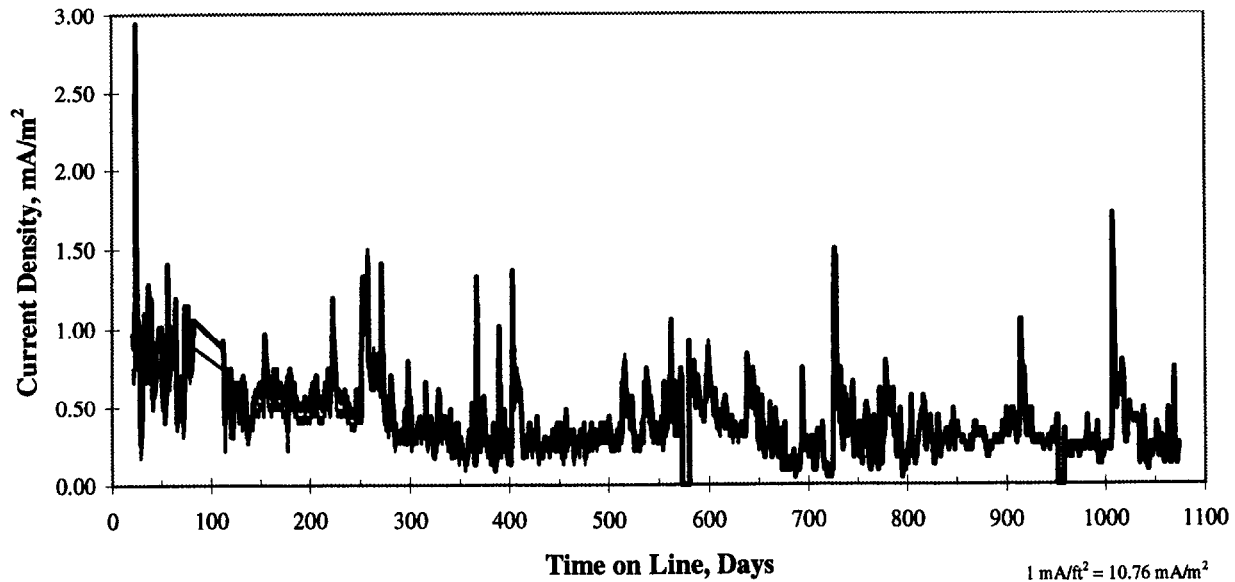


Figure 18. Current density versus time for metallized zinc anode system.

Table 5. Operating data for metallized zinc anode system.

Time on line, Months	0	10	17	25	38
Current, mA/m <sup>2</sup> *	1.6	0.5	0.2	0.2	0.2
Polarization Decay, mV*		252	205	315	216
Static Potential, mV versus Ag/AgCl*	-191	-115	-53	-21	-95
Anode-Cathode Resistance, Ω*	0.60	0.62		0.80	
Bond Strength, kPa**	860	1720	1660	1450	2590

\* Average of readings in both zones.

\*\* Measurements from zone 1.

Static potentials of the steel are also shown in table 5. Static potentials after start-up were recorded after 4 h of potential decay, even though potentials were still drifting positive at that time. From these data it is apparent that the application of cathodic protection current has resulted in steel potentials becoming more positive (more passive) with time. This is consistent with other experience, and is a result of the migration of chloride ions away from the steel and the build-up of hydroxide ions at the steel surface.

Anode-cathode resistance has changed little with time, perhaps increasing slightly over the test period, even though the total charge applied during this time was only 5.56 A-h/m<sup>2</sup> (0.516 A-h/ft<sup>2</sup>). Bond strength of the zinc anode to the concrete appears to have increased over the test period. This is consistent with the experience of other authors.<sup>(14)</sup>

The potentials of the steel, as monitored at the four embedded reference electrodes, are shown on figure 19. As shown on the figure, the operating potentials of all four embedded reference electrodes were roughly equivalent. These potentials are “current-on” potentials, since it was impossible to record “instant-off” potentials with the CP system operating in galvanic mode. The potentials are seen to become slightly less negative over the test period, a result of both the drift of static potential and the decrease of CP current with time. It is significant for this contract that the zinc operating in galvanic mode did not result in steel potentials sufficiently negative to cause hydrogen embrittlement.

#### Fiberglass Jacket/Titanium Mesh Anode System

Current requirement on the fiberglass jacket/titanium mesh anode system was established by the start-up tests as 5.16 mA/m<sup>2</sup> (0.48 mA/ft<sup>2</sup>). Based on the work of Bazzoni and Lazzari, it was decided to activate this zone in constant voltage mode of operation.<sup>(13)</sup> A voltage of 1.40 V was found to result in the required current, and the system was left at approximately that voltage for the duration of this contract. Figure 20 shows the voltage for the fiberglass jacket/titanium mesh anode zone to remain relatively constant during the entire monitoring period. The current for this zone, shown on figure 21, is seen to vary somewhat depending mainly on the ambient temperature variations of the seasons.

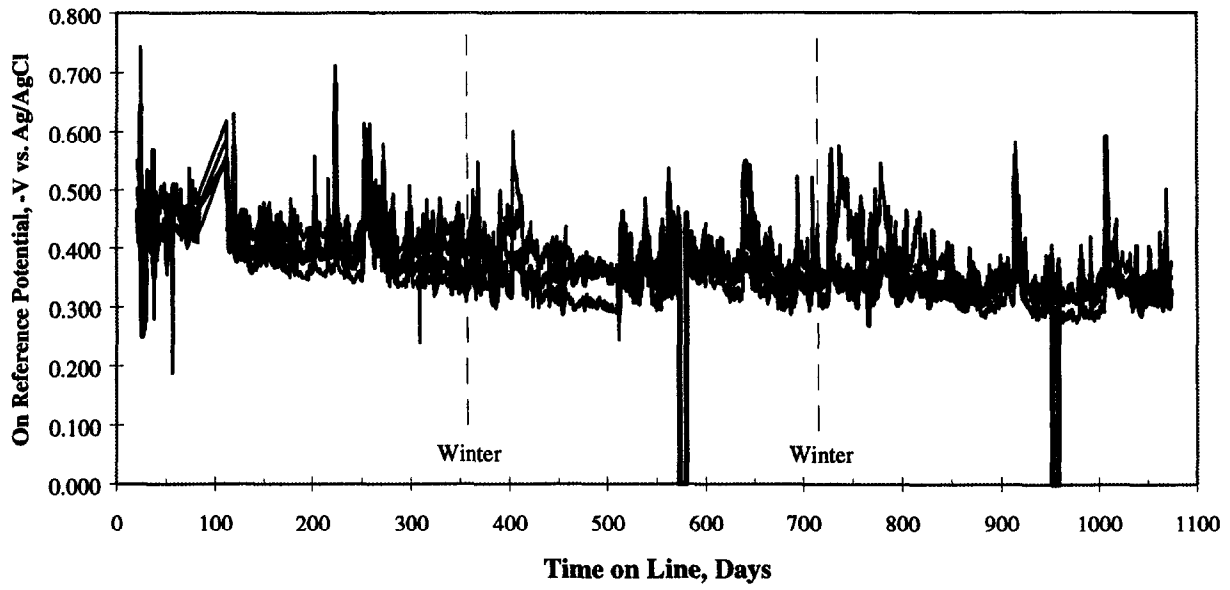


Figure 19. Potential versus time for metallized zinc anode system.

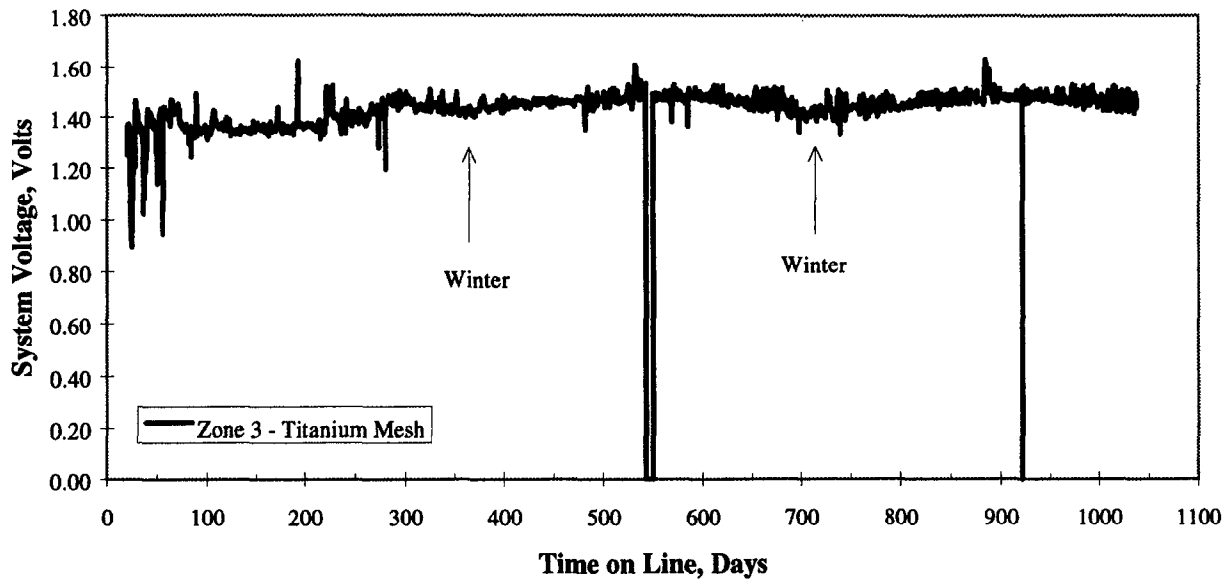


Figure 20. Voltage versus time for fiberglass jacket/titanium mesh anode system.

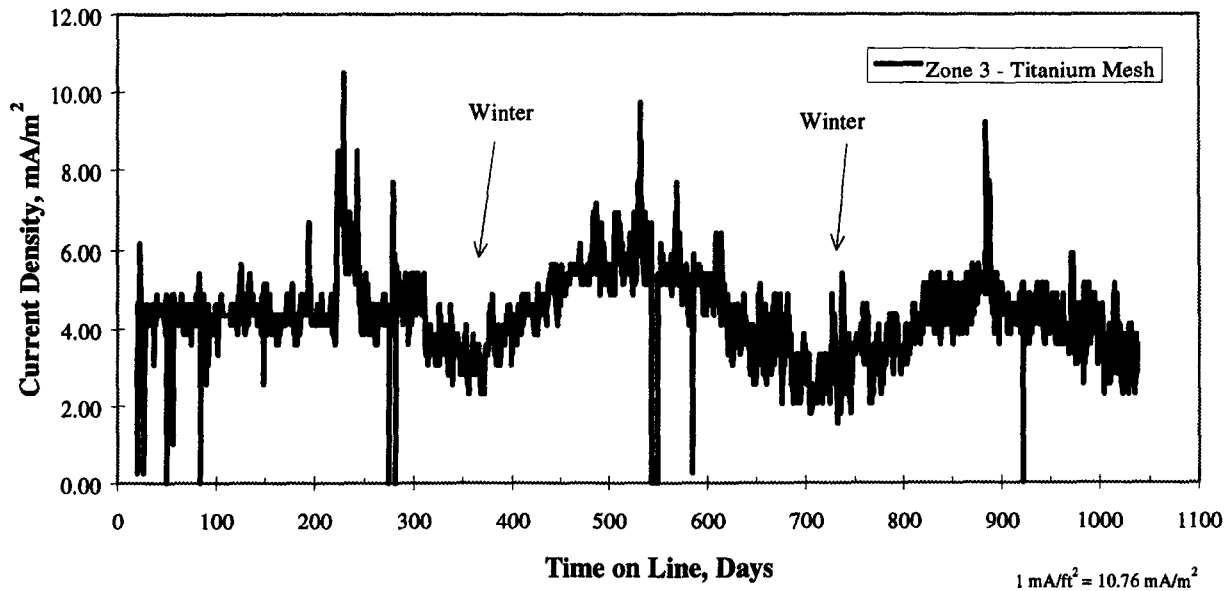


Figure 21. Current versus time for fiberglass jacket/titanium mesh anode system.

The voltages and current densities for the fiberglass jacket/titanium mesh anode system taken during the five scheduled monitoring visits are shown in table 6. Table 6 also shows results of the polarization decay testing conducted during these visits. Polarization decay is seen to generally exceed 100 mV, indicating that the applied current density was adequate. The instant-off potential taken during this testing shows that steel potentials were not more negative than -753 mV versus Ag/AgCl (-760 mV versus SCE). These results indicate that the steel in this zone was adequately protected from corrosion, while potentials at the surface of the steel were not sufficiently negative to cause hydrogen embrittlement. Anode-cathode resistance did not vary significantly during this time period.

Table 6. Operating data for fiberglass jacket/titanium mesh anode system.

Time on line, Months	0	10	17	25	38
Voltage	1.40	1.40	1.40	1.42	1.42
Current Density, mA/m <sup>2</sup>	5.6	4.2	5.3	2.9	3.1
Polarization Decay, mV		124	92 (158*)	(134*)	(130*)
Instant-Off Potential, (Ag/AgCl)	-378, -557	-635, -702	-672, -753	-426, -709	-592, -743
Anode-Cathode Resistance, Ω	0.37	0.33		0.36	

\* After 20 h of polarization decay, all other decay data after 4 h.

Potentials taken by remote monitor on the fiberglass jacket/titanium mesh anode system during this contract are shown on figure 22. Potentials are seen to be generally more negative during the summer months, a result of higher current densities in warm weather, but at no time did potentials exceed -840 mV versus Ag/AgCl (-847 mV versus SCE). These data again show that steel potentials were less negative than those required to cause hydrogen embrittlement during the entire monitoring period.

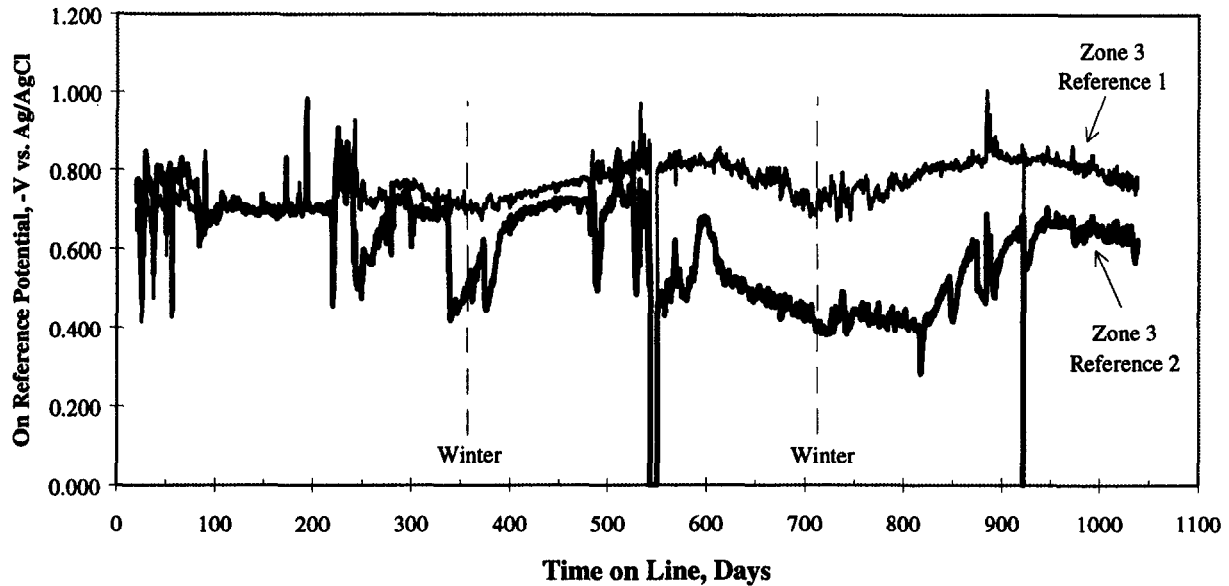


Figure 22. Steel potential versus time for fiberglass jacket/titanium mesh anode system

Another objective of testing this zone was to determine if the CP system could induce excessive (negative) potentials on the steel below seawater. This could be caused by current leakage to steel below water level. A relatively small amount of cathodic current could result in very negative potentials where the concrete is saturated, resulting in poor oxygen availability. Testing during each visit showed that the steel below seawater showed very little response to the operation of the fiberglass jacket/titanium mesh CP system. Leakage of current to seawater was effectively prevented by the fiberglass jacket and by the epoxy coating applied to the bottom of the grout. These components insulated the current path to seawater and served to direct current flow inward toward the steel beneath the anodes.

#### Conductive Rubber Anode System

Current requirement for the conductive rubber CP system could not be determined from the E-log I testing during system start-up. This was because the conductive rubber anode was directly exposed to the seawater at all times other than low tide. This direct contact between anode and seawater resulted in a low resistance path to steel in the piling below water level, and steel below water was quickly polarized to potentials more negative than -900 mV versus SCE during the E-log I test. Because of the uncertainty associated with this zone, it was decided to start-up this system at a conservative constant voltage of 1.0 V. The voltage for the conductive rubber CP system as taken and transmitted by the remote monitor is shown on figure 23. As shown on the figure, the power supply for this zone was not properly controlling voltage during the first 10 months of operation and system voltage was erratic, but this problem was corrected during the first scheduled visit. Following the first 10 months, the power supply properly controlled voltage at about 1.8 V during the winter. Voltage dropped during the summer months as the current limit of  $6.2 \text{ mA/m}^2$  ( $0.58 \text{ mA/ft}^2$ ) was reached.

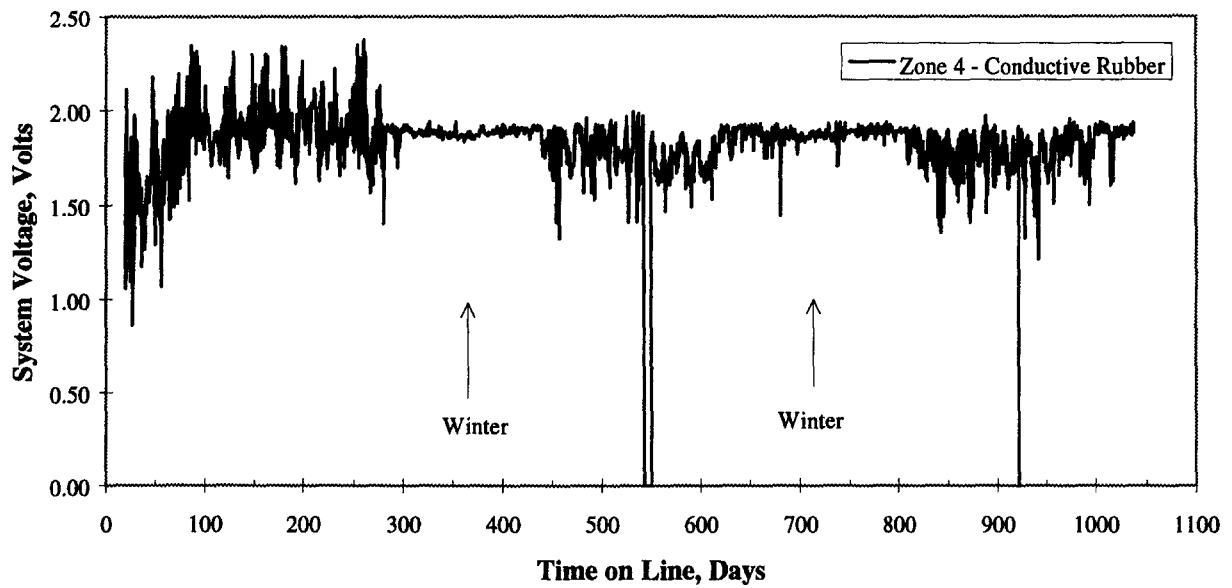


Figure 23. Voltage versus time for conductive rubber anode system.

Current density versus time for the conductive rubber anode CP system is shown on figure 24. Once again, current density is seen to increase during the summer months as a result of warm temperatures and lower electrolyte resistance. Current is seen to be much more erratic than that for the zone with titanium mesh anode. This is again a result of direct contact of the anode with seawater and current surges during periods of high tide.

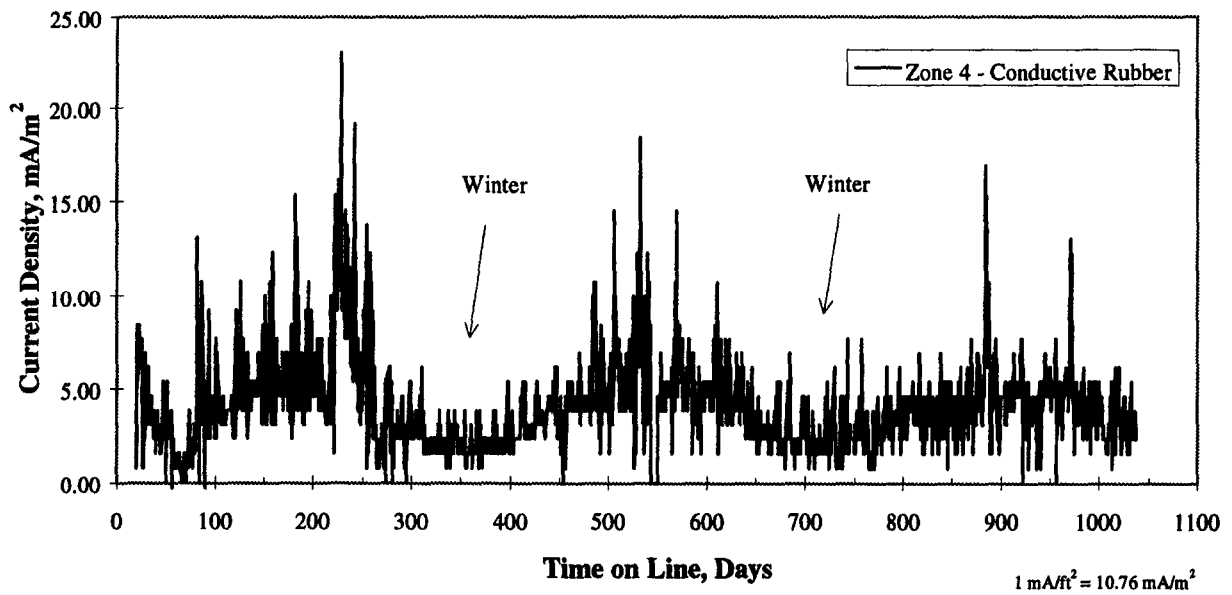


Figure 24. Current versus time for conductive rubber anode system.

Data taken during the five scheduled monitoring visits are shown on table 7. The most interesting information on table 7 is the polarization decay data. Polarization decay was found to be almost nonexistent after 4 h, and very small after 20 h. At no time was the accepted decay criterion of 100 mV observed for this system. But this does not necessarily mean that the steel in this zone was not being adequately protected. In fact, the IR-free potential of the steel showed it to be polarized about 200 mV more negative than the original static potentials. This apparent paradox is due to the fact that the conductive rubber anode is directly exposed to the seawater allowing current to freely flow to and from the submerged steel. Steel below water level quickly became polarized to about -820 mV versus SCE. When the rectifier current was interrupted, the submerged steel accepted current from steel in the splash and tidal zone, maintaining cathodic polarization of the steel beneath the anode. Because of this complex interaction, it may take several days, or even weeks, to observe complete polarization decay of the steel in this zone. This made criteria testing of this zone very difficult.

Table 7. Operating data for conductive rubber anode system.

Time on line, Months	0	10	17	25	38
Voltage	1.00	1.85	1.72	1.85	1.87
Current, mA/m <sup>2</sup>		1.5	5.0	2.1	3.8
Polarization Decay, mV		17	0 (44*)	(37*)	(57*)
Instant-Off Potential, (Ag/AgCl)	-316, -530	-512, -675	-512, -701	-434, -681	-523, -730
Anode-Cathode Resistance, Ω	2.4	2.0		3.2	

\* After 20 h of polarization decay, all other decay data after 4 h.

Potentials taken by remote monitor on the conductive rubber anode system during this contract are shown on figure 25. Potentials are again seen to be generally more negative during the summer months, a result of higher current densities in warm weather.

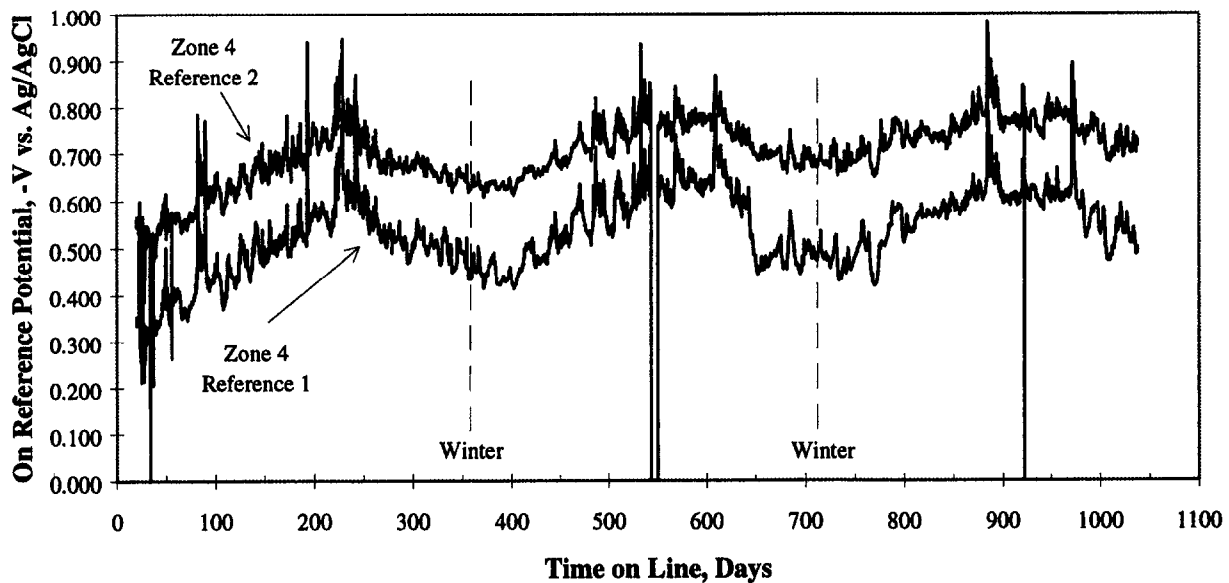


Figure 25. Steel potentials versus time for conductive rubber anode system.

Another interesting property of this zone is the relatively high anode-steel resistance. Even after adjusting for the smaller zone size, resistance is nearly three times that of the zone with titanium mesh anodes. It may be assumed that this additional resistance is in the contact between the anode and the concrete piling. The effectiveness of this contact is largely dependent on the presence of water at the anode-concrete interface. This causes some concern since the moisture content at that interface is inhomogeneous, varying with height above seawater. It therefore follows that a lower resistance at the bottom of the anode could cause excessive current densities in that area, raising concern about excessive polarization and hydrogen embrittlement. In order to investigate this problem, steel potentials were measured on selected pilings at the corners where concrete was exposed. The readings shown in table 8 were taken at low tide and are typical of several taken during the term of this contract.

The results reported in table 8 confirm high current densities and very negative steel potentials at the bottom of the conductive rubber anode. Potential measurements recorded on Pile #8 were especially negative, and actually exceeded the threshold for evolution of atomic hydrogen. These most negative potentials were not monitored remotely since the lowest embedded reference electrode was installed 0.46 m (1.5 ft) above the bottom of the anode jacket.

Table 8. Steel potentials on conductive rubber anode pilings as a function of elevation. (Potentials taken versus CSE reference electrode)

Elevation Above Bottom of Anode	Pile #1	Pile #2	Pile #4	Pile #7	Pile #8
1.22 m (4 ft)	-535	-454	-204	-419	-528
0.91 m (3 ft)	-630	-504	-239	-475	-827
0.61 m (2 ft)	-778	-646	-336	-694	-924
0.30 m (1 ft)	-903	-859	-569	-818	-1075
0 m (0 ft)	-892	-836	-783	-914	-1043
In Seawater			-874	-895	

## ABBEY ROAD BRIDGE

As reported in chapter 3, the metallized zinc anode on the Abbey Road Bridge was started up in galvanic mode of operation, and was left operating in galvanic mode for 6 months. But unlike the zones with metallized zinc on the Howard Frankland Bridge, the zinc at Abbey Road was not able to sustain sufficient current to adequately protect the steel. After 6 months the galvanic current density had dropped to only  $0.4 \text{ mA/m}^2$  ( $0.04 \text{ mA/ft}^2$ ). At this level of current, polarization decay at 13 different sites ranged from 10 mV to 115 mV and averaged only 43 mV. Polarization decay greater than 100 mV was recorded at only one site. This system was then re-energized in constant current mode at  $2.2 \text{ mA/m}^2$  ( $0.2 \text{ mA/ft}^2$ ). It was not immediately possible to operate this system in constant voltage mode since system voltage was very low.

The leakage of water between the joints of the box beams caused serious installation problems, as reported in chapter 3. Four months after start-up of the CP system, the Abbey Road Bridge was rehabilitated. The upper surfaces of the box beams were repaired, and a protective

membrane and new asphalt overlay were applied. Surprisingly, this rehabilitation did not entirely stop the joints from leaking, but confined the leaking to one joint. As the testing of this system continued, it became apparent that this leaking joint presented a serious operational problem.

The data taken 15 months after start-up and presented on table 9 are typical of data taken at Abbey Road throughout this contract. Table 9 presents data from a 4-h polarization decay test. Potentials are taken at the two embedded reference electrodes, at windows in each of the ten beams, and at potential wells installed in Beam #3 and Beam #9.

As shown on table 9, four of the instant-off potentials recorded were sufficiently negative to evolve atomic hydrogen (potentials highlighted by bold format). This would indicate that current density is too high, and that current should be reduced. But the polarization decay data indicate that the 100 mV polarization decay criterion was not achieved at 6 out of 15 sites (those highlighted by bold format). This would normally indicate that the current should be increased. This conflict is caused by the inhomogeneous nature of this structure. Based on these data, it appears to be impossible to adequately protect all sites from corrosion, while at the same time avoiding potentials sufficiently negative to evolve hydrogen and possibly cause hydrogen embrittlement.

Table 9. Potential decay test at Abbey Road Bridge after 15 months of operation.

Test Location	Instant-Off Potential, mV	Potential After 4 h, mV	Polarization Decay, mV
Embedded Ref. #1	-480	-343	137
Embedded Ref. #2	-362	-289	<b>73</b>
Beam 1	-145	-54	<b>91</b>
Beam 2	-282	-204	<b>92</b>
Beam 3	-423	-243	180
Beam 4	-282	-228	<b>66</b>
Beam 5	-825	-394	431
Beam 6	<b>-1042</b>	-652	537
Beam 7	<b>-1252</b>	-736	789
Beam 8	-656	-517	237
Beam 9	<b>-1070</b>	-553	566
Beam 10	-240	-178	<b>62</b>
Well in Beam #3	-388	-313	<b>75</b>
Well in Beam #9	<b>-1892</b>	-819	1073
Next to Beam #9 Well	-893	-680	213

Following these tests, this CP system was converted to voltage control, and a voltage was selected that resulted in lower average current density. At the next scheduled test, average current density was only 0.65 mA/m<sup>2</sup> (0.06 mA/ft<sup>2</sup>) at a system voltage of 1.16 V, and the number of sites where potentials were sufficiently negative to evolve hydrogen were down to two. But the number of sites where the 100 mV polarization decay criterion was not achieved

was up to 11. Even after waiting 7 days after current-off, the 100-mV criterion was still not achieved at 4 sites. This problem persisted throughout the monitoring period, as shown on table 10.

Table 10. Summary of operating data from Abbey Road Bridge.

Time on line, Months	0	15	19	26	30
Voltage	Galvanic	1.20	1.16	1.16	1.17
Current, mA/m <sup>2</sup>	5.3	2.7	0.6	1.2	0.8
Potential >H <sub>2</sub> Threshold, no. of sites	-	4 (27%)	2 (13%)	2 (13%)	1 (7%)
Potential Decay <100 mV, no. of sites	-	6 (40%)	11 (73%)	11 (73%)	11 (73%)
Bond Strength, kPa	1550	3860		3730	2550
Anode-Cathode Resistance, Ω	0.26	0.24	0.30	0.30	0.29

It is also likely that the bond strength between the zinc anode and the concrete increased with charge, as was the case for the zinc anode applied to the Howard Frankland Bridge. These data are also shown on table 10, although the number of samples taken were insufficient for statistical accuracy. As also shown on table 10, the anode-cathode resistance remained constant over the first 30 months of operation.

A malfunction of the RMU prevented remote gathering and transmitting of data at the Abbey Road Bridge over the entire monitoring period. Troubleshooting early in the contract failed to correct the problem, and the problem persisted even after complete exchange of the RMU for a new unit. Data were collected and transmitted, but were inaccurate. This was likely due to some interference, which remained unidentified throughout the period.

Because of the disparity of current density on this structure, an attempt was made to map the current distribution in September 1996. The mapping was conducted by Dr. R. Shrinivasan of Johns Hopkins University, and was done using two magnetic sensors that measure the magnetic field generated by the electric current on the bridge. The results of this mapping did not show high current density at the leaking joints, but did indicate high current density concentrated around the power feed points on Beams #5 and #6. This conclusion was not substantiated by any other data, and was difficult to rationalize since the IR-drop in the zinc anode was practically nil. Despite these reservations, it was decided to test the prestressing steel in Beams #5 and #6 at the conclusion of the monitoring period for hydrogen content and hydrogen embrittlement.

#### WEST 130<sup>TH</sup> STREET BRIDGE

The West 130<sup>th</sup> Street Bridge, like the Abbey Road Bridge, was characterized by leaking joints between adjacent box beams. Since this bridge was not superelevated, wetness was confined to the immediate area of the joint, but there was still concern that this condition would lead to large localized variations in resistance and current density. The wettest beams were Beams #1 through #4 and Beam #14. These were the beams located beneath the curb areas of the bridge, and where the drainage scuppers were located.

A slow, incremental start-up was recommended by the manufacturer of the conductive paint anode to ensure acceptable bonding of the anode to the concrete. Slow start-up was also considered prudent in view of the leaking joints and the nonhomogeneous nature of the structure. The system was energized at  $2.15 \text{ mA/m}^2$  ( $0.2 \text{ mA/ft}^2$ ) on May 26, 1994. After 13 days of operation, the current was raised to  $4.3 \text{ mA/m}^2$  ( $0.4 \text{ mA/ft}^2$ ), and after an additional 7 days was raised to  $6.45 \text{ mA/m}^2$  ( $0.6 \text{ mA/ft}^2$ ). No E-log I testing was conducted since it was feared that the high current densities needed to complete the test could harm the anode.

After less than 2 months of operation, anode disbondment in the form of hundreds of small blisters was noticed. These blisters were generally less than 20 mm in diameter, were concentrated in wet areas of the beams, and most were liquid-full. No pattern was found relative to distance from the power feed points. The reason for this early disbondment is not known, but may possibly be related to a few spikes of current the anode experienced during the first few days of operation. During this time the rectifier apparently malfunctioned, failing at times to control in constant current mode. The reason for this rectifier malfunction is not known.

After about 2 months of operation, the rectifier was placed in constant voltage control mode and operated properly for the remainder of the contract. Over the remaining months of operation under this contract the disbondment of the anode did not progress further, and at the conclusion of the monitoring period the anode continued to remain bonded and provide adequate current for corrosion control. The amount of anode represented by the disbonded blisters is estimated at not more than 5 percent of the total area.

The first polarization decay testing was conducted after about 2 months of operation. Even though the current density was low prior to the test,  $6.45 \text{ mA/m}^2$  ( $0.6 \text{ mA/ft}^2$ ), steel potentials were very negative and polarization decay values were very high. Thirteen out of 19 instant-off potentials were sufficiently negative to evolve hydrogen. The average polarization decay was 724 mV, and the 100 mV criterion was exceeded at all 19 sites. It was clear that, despite the fairly low current density, the steel in this structure was being strongly overprotected and that hydrogen embrittlement was a possibility. The power supply was then placed in constant voltage mode at about 2.8 V, which reduced the current density to  $3.23 \text{ mA/m}^2$  ( $0.3 \text{ mA/ft}^2$ ).

The system was left operating at this voltage until 14 months of time on line. At that time a second polarization decay test was conducted, and the results of that test are shown in table 11.

Table 11. Potential decay test at West 130<sup>th</sup> Street Bridge after 14 months of operation.

Test Location	Instant-Off Potential, mV	Potential After 4 h, mV	Polarization Decay, mV
Embedded Ref. #1	-936	-585	351
Embedded Ref. #2	-650	-476	174
Beam 1	-920	-475	445
Beam 2	<b>-1057</b>	-612	445
Beam 3	-885	-476	409
Beam 4	<b>-1120</b>	-565	555
Beam 5	-932	-330	602
Beam 6	-916	-251	665
Beam 7	<b>-1023</b>	-121	902
Beam 8	-895	-274	621
Beam 9	-820	-185	635
Beam 10	-805	-282	523
Beam 11	<b>-1100</b>	-660	440
Beam 12	-898	-277	616
Beam 13	-779	-294	485
Beam 14	<b>-1081</b>	-887	194
Beam 15	-748	-389	359
Well in Beam #2	<b>-1019</b>	-731	288
Well in Beam #12	-852	-507	345

It is obvious from the data in table 11 that the steel was still being overprotected at the time of this test. Instant-off potentials sufficiently negative to generate hydrogen were recorded at six sites. The average polarization decay was 453 mV, and the 100 mV criterion was exceeded at all 19 sites. The constant voltage control was then reduced to 2.2 V, which resulted in a current density of about 2.15 mA/m<sup>2</sup> (0.2 mA/ft<sup>2</sup>). Data taken during the scheduled monitoring tests for the West 130<sup>th</sup> Street Bridge are summarized in table 12.

Table 12. Summary of operating data from West 130<sup>th</sup> Street Bridge.

Time on line, Months	2	14	24	28
Voltage	3.40	2.86	2.15	2.29
Current, mA/m <sup>2</sup>	6.46	3.12	1.18	1.18
Potential >H <sub>2</sub> Threshold, no. of sites	13 (68%)	6 (32%)	0 (0%)	0 (0%)
Potential Decay <100 mV, no. of sites	0 (0%)	0 (0%)	9 (47%)	8 (47%)
Bond Strength, kPa	860	860	1550	1240
Anode-Cathode Resistance, Ω	0.57	-	0.71	0.70

This table shows a record of the effort to find a level of cathodic protection that would result in safe operating potential of the steel (less negative than the potential at which hydrogen would be evolved), yet which would meet accepted CP criteria. As with the Abbey Road Bridge, it was not possible to accomplish both objectives. The data recorded at 24 and 28 months of

operation showed all instant-off potentials slightly less negative than potentials need to evolve hydrogen, but in both cases many sites did not meet the 100-mV polarization decay criterion. Following the test conducted at 28 months, the system was left to depolarize for 4 days, and three of the sites still had not met the 100-mV criterion. This inability to both operate at safe potentials and meet CP criteria was apparently due to the nonhomogeneous nature of the structure, which in turn led to a large disparity in current densities and steel potentials.

A record of the operating voltage and current density versus time is shown in figures 26 and 27, respectively. In both figures, the failure of the power supply to control constant current during the first 2 months of operation can be plainly seen.

A record of embedded reference potentials with time is shown on figure 28. Potentials shown are current-on potentials. Instant-off potentials were determined to be about 100 to 140 mV less negative than those shown on the figure.

The bond strength of the conductive paint anode at the West 130<sup>th</sup> Street Bridge was highly variable, ranging from 2070 kPa (300 lb/in<sup>2</sup>) in some areas to zero in others. Bond strength was lowest in those areas where blisters had formed. There appeared to be no relationship between bond strength and distance from the power feed points.

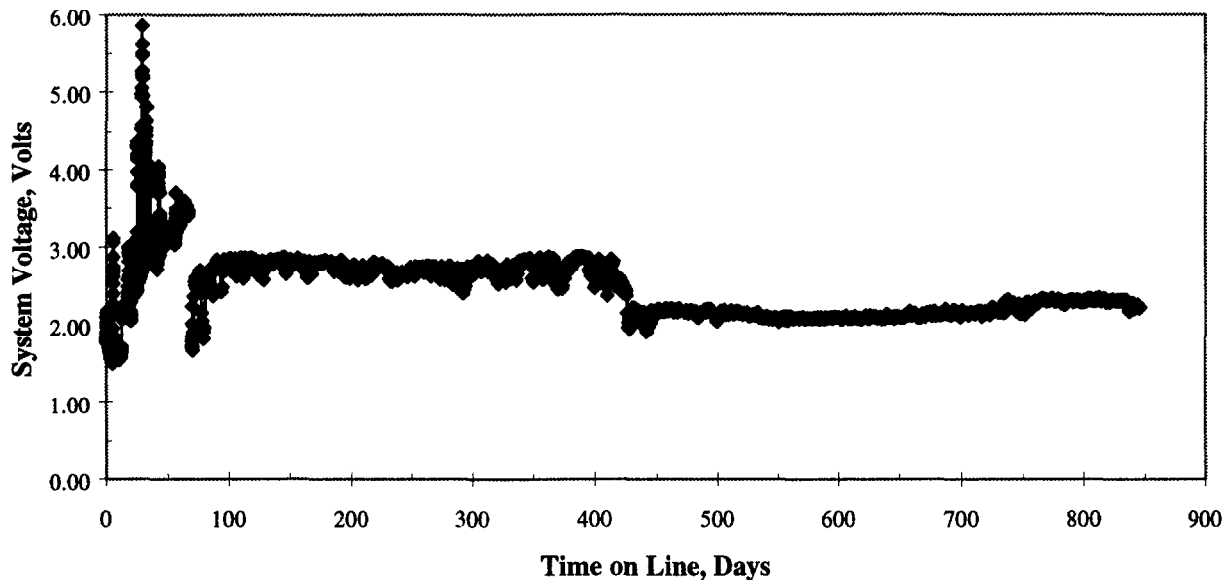


Figure 26. Voltage versus time for West 130<sup>th</sup> Street Bridge.

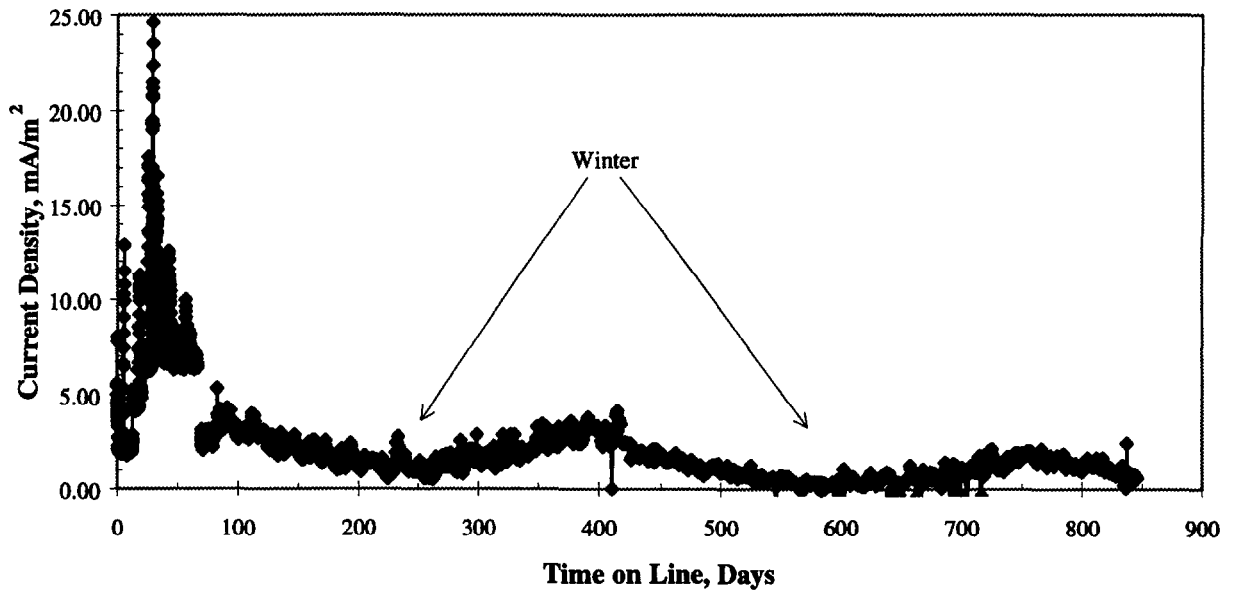


Figure 27. Current versus time for West 130<sup>th</sup> Street Bridge.

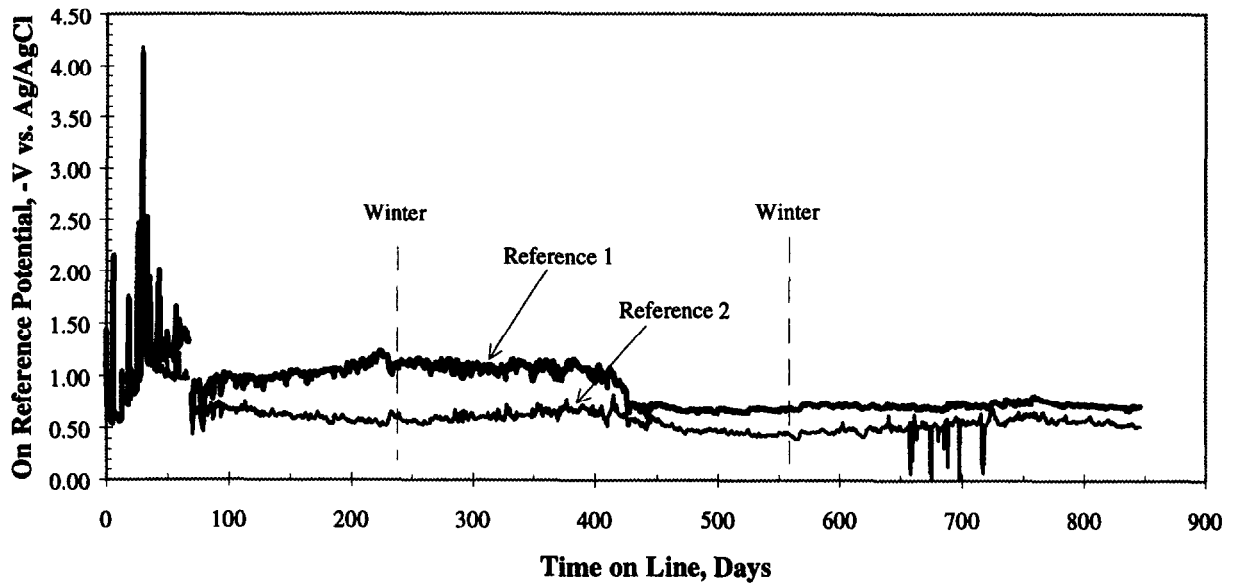


Figure 28. Steel potentials versus time for West 130<sup>th</sup> Street Bridge.

## EMBEDDED HYDROGEN PROBES

Hydrogen probes were embedded in each of the structures studied under this contract. The probes selected were sealed Devanathan cells developed for field use by the Danish Corrosion Center (FORCE Institute). A thin sheet of steel at one end of the probe was polarized together with the reinforcement. If hydrogen enters this probe, it diffuses through the steel sheet and becomes oxidized at the inner surface, which is held at a high potential by an internal counter electrode. An increase in current over the background current represents the permeation current, which is proportional to the hydrogen flux through the steel sheet. In this way, it was hoped that overprotection which results in the generation of atomic hydrogen would be immediately sensed. Hydrogen probes were embedded at most anodic sites.

The response of the hydrogen probes was monitored during start-up of the cathodic protection systems installed on the Howard Frankland Bridge. For zones 1, 3, and 4, hydrogen probe response was minimal throughout the test. But for the hydrogen probe in zone 2, a significant response was recorded as current was increased. The hydrogen probe in this zone began responding when the steel potentials, as measured by the embedded reference electrodes, were only -223 and -97 mV versus silver/silver chloride. Throughout this contract, it appeared that a response from the hydrogen probes were not a true indication of atomic hydrogen production. Similar observations were made for the hydrogen probes installed on the bridges in Ohio. Probes frequently showed a response at potentials far too positive to permit hydrogen evolution, and at other times failed to indicate a response when potentials were very negative. The reason for the lack of success with the Devanathan probes is not known.



## CHAPTER 5. POST-MONITORING ANALYSES OF CONCRETE AND STEEL

### ACQUISITION OF SPECIMENS

Specimens were taken from four locations on the Abbey Road Bridge on November 1, 1996. Locations were selected that would be most likely to experience hydrogen embrittlement (according to recorded steel potentials), as well as locations unlikely to experience embrittlement. At least one 10.2-cm- (4-in-) diameter core, and one 0.64-m- (25-in-) long sample of prestressing strand was removed from each of the four locations. The cores were sent to Lankard Materials Laboratory for analysis of quality of bond and concrete integrity. The long samples of prestressing strand were packed in dry ice and shipped to Florida Atlantic University for determination of hydrogen content and mechanical properties.

The specimens taken from Abbey Road Bridge include the following:

Beam #2, west joint (dry), about 1 m (3 ft) from the north end of the span. This location was generally dry, did not experience high current densities, and did not operate at very negative potentials. The specimen was taken only minutes after current-off, and was placed immediately in dry ice to prevent out-gassing.

Beam #5, west joint (dry), about 1 m (3 ft) from the south end of the span. This location was generally dry, did not experience high current densities, and did not operate at very negative potentials, but was identified as an area of high current density by Dr. R. Shrinivasan of Johns Hopkins University. The specimen was taken about 0.5 h after current-off and was placed immediately in dry ice.

Beam #6, west joint (dry), about 1 m (3 ft) from the south end of the span. This location was generally dry, did not experience high current densities, and did not operate at very negative potentials, but was identified as an area of high current density by Dr. R. Shrinivasan of Johns Hopkins University. The specimen was taken about 1 h after current-off and was placed immediately in dry ice.

Beam #9, west joint (wet), about 1 m (3 ft) from the south end of the span. This location was generally wet and frequently experienced high current densities and very negative operating potentials. The specimen was taken about 1.5 h after current-off and was placed immediately in dry ice.

All cavities left by the removal of specimens were patched with Emacco S-88 grout in May, 1997.

It was decided not to take specimens from the West 130<sup>th</sup> Street Bridge, but rather additional specimens were taken from the Abbey Road Bridge because of the extreme disparity of current density on that structure.

Specimens were taken from the Howard Frankland Bridge on March 25, 1997. Here it was decided to remove specimens from pilings with conductive rubber near the bottom of the anode, since this area had experienced very negative potentials during the monitoring phase of the contract. Specimens were not removed from the girders protected by metallized zinc anodes since current densities there were low and potentials relatively positive. Specimens were not removed from pilings protected by titanium mesh anodes since potentials there were less negative than the piles with conductive rubber, and because of the difficulty of sampling beneath the fiberglass jackets and grouting. Two 5-cm- (2-in-) diameter cores, and one 0.51-m- (20-in-) long sample of prestressing strand was removed from each piling. The cores were sent to Lankard Materials Laboratory for analysis of quality of bond and concrete integrity. The long samples of prestressing strand were packed in dry ice and shipped to Florida Atlantic University for determination of hydrogen content and mechanical properties.

The specimens taken from the pilings on the Howard Frankland Bridge include the following:

Piling #7, near the bottom of the anode. This location generally experienced very negative operating potentials. Specimens were taken about 2 h after current-off, and placed immediately in dry ice to prevent out-gassing.

Piling #8, south piling, near the bottom of the anode. This location generally experienced very negative operating potentials. Specimens were taken about 3 h after current-off, and placed immediately in dry ice to prevent out-gassing.

Following the sampling, the prestressing steel was tested and found to be electrically continuous, and all cavities were repaired with Emaco S-88 grout.

## HYDROGEN CONTENT AND MECHANICAL PROPERTIES OF STEEL

### Experimental Procedure

The procedure for hydrogen analysis involved measurement of the total charge density transferred (current density versus time) as a 45-mm wire length was maintained at a potential of +0.060 V (SCE) in a deaerated 0.2 M NaOH solution. Four types of specimens from each of the tendon samples were tested, as listed below:

1. Spiraled outer tendon wire.
2. Straight center tendon wire.
3. Spiraled outer tendon wire that had been straightened by tensile elongation.
4. Spiraled outer wire that had been heated to 300 °C for 3 h.

It was anticipated that no electrochemical reduction should occur on the center, straight wire (category 2 above) since it did not have direct contact with the electrolyte (concrete). Accordingly, it should not contain any dissolved hydrogen that might have otherwise resulted

from cathodic protection. Similarly, any hydrogen in the heated wires (category 4) is expected to have outgassed. Thus, it was intended that these two specimen types (2 and 4) serve as controls. Alternately, any difference in hydrogen concentration between the former two specimen types and ones in test category 1 should provide a measure of hydrogen which accumulated in the steel in association with cathodic protection. Specimens in test category 3, on the other hand, were mechanically straightened as a precursor to strength testing, as explained below, and data from these should provide information regarding any effect of this upon hydrogen concentration. The current density versus time data from the individual tests were recorded via a data acquisition system, and the area under the resultant curve was integrated using a statistical program. Because samples in all four categories exhibited a finite charge transfer during the time of anodic polarization, the charge transfer for the category 4 samples was averaged, and this value was subtracted from that for the other specimens. The finding that charge was transferred for category 3 and 4 samples was attributed to either: (1) residual hydrogen in the steel or (2) residual oxidant in the electrolyte or to some combination of these. The hydrogen concentration was calculated on the basis that 1 Coulomb corresponds to  $1.045 \times 10^{-5}$  grams of hydrogen.

Constant Extension Rate Testing (CERT) was selected as the technique for evaluating the mechanical properties and any embrittlement tendency of the tendon wires. This was done at an extension rate of  $4.7 \times 10^{-5}$  mm/s using the same instrumentation and procedure that has been previously utilized in this laboratory. Testing was performed in air at room temperature and took approximately 11 hours. Specimen preparation involved the following steps:

1. The length of each spiraled wire to be tested was extended at a rate of 0.15 mm/s in a tensile testing machine until it was straight.
2. Straightened wires were machined by centerless grinding to provide a reduced section gauge length. A refrigerated coolant was passed across the specimen during this process, and grinding was performed at a slow speed to minimize local heat generation.

Subsequent to testing, the data were analyzed, and strength and ductility were determined.

#### Abbey Road Bridge

Samples of prestressing wire from the Abbey Road Bridge were received, packaged, and shipped in dry ice, at the Florida Atlantic University Materials and Corrosion Laboratory on November 5, 1996. These included specimens from Beam #2, Beam #5, Beam #6, and Beam #9. Each specimen was sectioned into 250-mm lengths with one-half of these being available for hydrogen concentration determination and the second half for mechanical property measurement. During storage and wherever possible during the test program, the samples were maintained in dry ice (inadvertently, the packaging dry ice expired on one occasion at which time the samples from Abbey Road Bridge are thought to have been at room temperature for as long as several hours).

Table 13 provides a summary of the hydrogen content and concentration as determined according to the procedure described above.

Table 13. Hydrogen content data from Abbey Road Bridge samples.

Specimen	Wire description	Hydrogen content, g	Hydrogen content, wt. %
Beam #2	Outer wire	$4.75 \times 10^{-6}$	$6.87 \times 10^{-5}$
“	Center wire	$9.50 \times 10^{-7}$	$1.86 \times 10^{-5}$
“	Stretched	$1.63 \times 10^{-6}$	$3.39 \times 10^{-5}$
Beam #5	Outer Wire	$3.19 \times 10^{-6}$	$6.67 \times 10^{-5}$
“	Center wire	$2.74 \times 10^{-6}$	$5.37 \times 10^{-5}$
“	Stretched	$1.91 \times 10^{-6}$	$3.97 \times 10^{-5}$
Beam #6	Outer wire	N*	N*
Beam #9	Outer wire	N*	N*

N\* - Not significantly greater than controls.

The test data showed that the hydrogen contents of Beam #6 and Beam #9 were not significantly greater than that of the controls. This is somewhat surprising since very negative potentials were recorded on Beam #9 throughout the monitoring period, and it had been proposed from current density mapping tests that Beam #6 had experienced high current densities. The highest hydrogen content was recorded on Beam #2, which was predicted from all available data to have no hydrogen content. The hydrogen contents recorded for Beam #2 and Beam #5 were relatively small, although large enough to cause a reduction in ultimate tensile strength for notched Grade 270 tendon wire according to Enos, et al.<sup>(9)</sup>

The CERT test results for the Abbey Road Bridge indicated no significant difference, first, among the different specimen types (annealed, center, or untreated wires) and, second, among the four tendon samples. For example, the average ultimate tensile strengths (UTS) for these specimens were 1730 MPa (251 kip/in<sup>2</sup>), 1850 MPa (268 kip/in<sup>2</sup>), 1760 MPa (255 kip/in<sup>2</sup>) and 1740 MPa (252 kip/in<sup>2</sup>), respectively for the wire samples from Beams #2, #5, #6, and #9. UTS for the annealed, center, and untreated samples averaged 1732 MPa (251 kip/in<sup>2</sup>), 1770 MPa (257 kip/in<sup>2</sup>), and 1743 MPa (253 kip/in<sup>2</sup>), respectively. All of these values fall below the minimum specified UTS for Grade 270 tendon (1863 MPa [270 kip/in<sup>2</sup>]), although they are above the minimum value for Grade 250 material (1725 MPa [250 kip/in<sup>2</sup>]).

#### Howard Frankland Bridge

The specimens that had been removed from substructure pilings of the Howard Frankland Bridge in Tampa, Florida, were received at Florida Atlantic University on March 27, 1997. Each tendon was labeled “top” and “bottom” and “sea water” and “pile,” where the former refers to the upward versus submerged orientation of the tendon and the latter to that face which projected toward the environment as opposed to toward the piling interior. Both tendon samples were sectioned into three 170-mm (6.7-in) lengths with the uppermost section being labeled “A,” the middle “B,” and the bottom “C.” Labels were instituted in an attempt to identify those locations where cathodic polarization was likely to have been highest (environment facing portion of the specimen) so that the analyses for hydrogen and any embrittlement could take this into account. The tendons were packaged in dry ice when received and, except for handling, preparation, and testing, were maintained in dry ice thereafter.

Except for three specimens, there were no significant differences in the hydrogen content for samples from the Howard Frankland Bridge, ranging from  $1.06 \times 10^{-5}$  to  $3.88 \times 10^{-5}$  weight percent. But higher hydrogen content was recorded for three specimens, which ranged from  $1.26 \times 10^{-6}$  to  $5.98 \times 10^{-6}$  weight percent. Of those three specimens, one was from pile #7 and two were from pile #8; one faced seaward, one inward, and one midposition; one was positioned at the top, one bottom, and one midrange. No significant trend could be detected relating hydrogen content to any other variable, nor did the hydrogen content appear to relate to any measured mechanical properties.

A summary of the CERT data taken on samples from the Howard Frankland Bridge is presented in table 14.

Table 14. CERT results for Howard Frankland Bridge samples.

Specimen	Yield stress, MPa (kip/in <sup>2</sup> )	Maximum stress, MPa (kip/in <sup>2</sup> )	Fracture stress, MPa (kip/in <sup>2</sup> )	Strain to fracture, %
Pile #7, top	1820 (264)	1970 (286)	1568 (227)	4.9
Pile #7, mid	1680 (243)	1780 (258)	1409 (204)	4.0
Pile #7, bottom	1670 (242)	1830 (265)	1401 (203)	4.4
Pile #8, top	1820 (264)	1960 (285)	1464 (212)	4.2
Pile #8, mid	1810 (263)	1930 (280)	1512 (219)	4.2
Pile #8, bottom	1760 (255)	1930 (280)	1492 (216)	4.7

As shown on table 14, the average UTS for tendon #8 samples from each of the three elevations was essentially the same (1960 MPa (285 kip/in<sup>2</sup>), 1930 MPa (280 kip/in<sup>2</sup>), and 1930 MPa (280 kip/in<sup>2</sup>) for elevations A, B, and C, respectively). Correspondingly, the UTS for tendon #7 wires at elevation A (highest) was 1965 MPa (285 kip/in<sup>2</sup>); however, the UTS at the B and C elevations was 1780 MPa (256 kip/in<sup>2</sup>) and 1830 MPa (265 kip/in<sup>2</sup>), respectively. These latter values are consistent with greater polarization at the lower elevations having affected more negative polarization and strength reduction. However, this finding can not be correlated with any difference in hydrogen concentration or any other variable.

Based upon CERT results and hydrogen concentration determinations for notched Grade 270 tendon wire specimens, it was concluded that UTS decreased progressively once the hydrogen concentration exceeded  $6.35 \times 10^{-6}$  weight percent. However, since the maximum UTS reduction for smooth specimens has been found to be 10 percent under conditions of even extreme cathodic polarization ( $E < -1.20$  versus SCE), the hydrogen concentrations for the present samples, which often exceeded the above threshold value, do not necessarily translate to significantly reduced strength. The finding that ductility of all the specimens was relatively high (typically 4 to 5.5 percent) is consistent with little or no embrittlement having occurred.

## QUALITY OF BOND AND INTEGRITY OF CONCRETE

### Experimental Procedure

The post-cathodic protection samples were examined by Lankard Materials Laboratory, Inc., to determine the effect of the CP treatment on the integrity of the concrete surrounding the prestressing steel and on the quality of the bond between the concrete and the steel. The techniques used to evaluate these effects are documented in a previous study that involved the post-CP analysis of concrete samples taken from eleven 18- to 32-year-old reinforced concrete bridge and parking structures that were under cathodic protection for 2 to 10 years.<sup>(15)</sup> Assessments were made using standard petrographic examination procedures (ASTM C-856<sup>(16)</sup>), and using scanning electron microscope (SEM) and energy dispersive X-ray spectroscopy (EDS) procedures. The parameters used in evaluation of the post-CP concrete samples include:

1. Assessment of the physical condition of the concrete in direct contact with the prestressing steel (color, hardness, texture).
2. Assessment of the physical condition of the concrete immediately adjacent to the prestressing steel.
3. Assessment of the physical condition of concrete at distances greater than 5 mm (0.2 in) from the prestressing steel.
4. Assessment of the contact zone (bond) between the prestressing steel and the concrete.
5. Assessment of the microstructure of the concrete in contact with the prestressing steel compared with the microstructure of concrete not in contact with the steel (SEM).
6. Assessment of the chemistry of the concrete in contact with the prestressing steel compared with concrete not in contact with the steel (EDS).
7. Assessment of the pH and extent of carbonation of the concrete in contact with the prestressing steel (application of indicating solutions on freshly exposed surfaces).

The concrete samples from the Abbey Road Bridge all contained prestressing steel making it possible to apply all of the parameters just described. The concrete samples from the Howard Frankland Bridge structure contained steel surfaces in the concrete, but none of the prestressing steel remained in the samples. All of these contact surfaces had therefore been exposed to the elements prior to examination at Lankard Materials Laboratory, eliminating the possibility of some of the evaluation steps (4 and 7).

## Abbey Road Bridge

Figure 29 shows photographs of one of the cores from Beam #6 of the Abbey Road Bridge in as-received condition at Lankard Materials Laboratory. This core was typical of cores from this bridge. The groove in the surface of the soffit was cut to limit the flow of water leaking through a joint. The concrete represented by the Abbey Road Bridge samples was characterized as an air-entrained portland cement containing a 2.5-cm (1.0-in) nominal maximum size crushed gravel coarse aggregate and a natural sand. In all cases, the concrete was well consolidated showing no abnormal amounts of gross porosity and no honeycomb. Both the coarse and the fine aggregate contained both carbonate and siliceous rock types. All of the Abbey Road Bridge samples were air-entrained with an average air content of 5 to 6 percent. The cementitious phase in the concrete was comprised solely of well hydrated portland cement. The water-cement ratio (w/c) of the concrete was estimated at 0.40 to 0.44. For the age and w/c of this concrete, there is a normal amount of unhydrated cement.

Figure 30 shows typical optical microscope views of the cross section of the 7-wire prestressing steel strand in the sample from Beam #9. The steel/concrete bond surface was examined in both planar and section orientations using optical microscopy and SEM examinations. A second procedure to provide physical characterization of the prestressing steel/concrete bond involved purposeful fracture of the concrete along its contact surface with the prestressing steel. This procedure provided the opportunity for a complete inspection of all surfaces of the prestressing wires, as well as all surfaces in contact with the prestressing steel.

Figure 31 shows optical microscope views of the features just discussed. The top photograph shows the concrete contact surfaces with the prestressing strands in the sample from Beam #2. The concrete surfaces in contact with the prestressing steel comprised a dense, compact surface of hydrated portland cement showing small amounts of porosity (entrained air voids). Concrete surfaces in contact with the prestressing steel were typically free of steel corrosion products. However, occasional light staining of the surface with corrosion products was not uncommon. Infrequently, a moderate amount of steel corrosion product was present in the concrete surface contacting the steel. Samples from Beams #6 and #9 showed moderately more corrosion than samples from Beams #2 and #5.

The bottom photograph in figure 31 shows prestressing steel wires still in place in the concrete alongside concrete from which the prestressing wire had been removed. The steel surfaces shown here were those defining the interior of the prestressing strand bundle. In all of the Abbey Road Bridge samples examined, there was very little penetration of the concrete into the interior of the steel wire strand. Interior steel surfaces not in contact with concrete typically show light corrosion such as that shown in the bottom photograph of figure 31. The overall condition of the prestressing wires in all of the cores examined here following the CP treatment was characterized as excellent with virtually no loss of steel section.

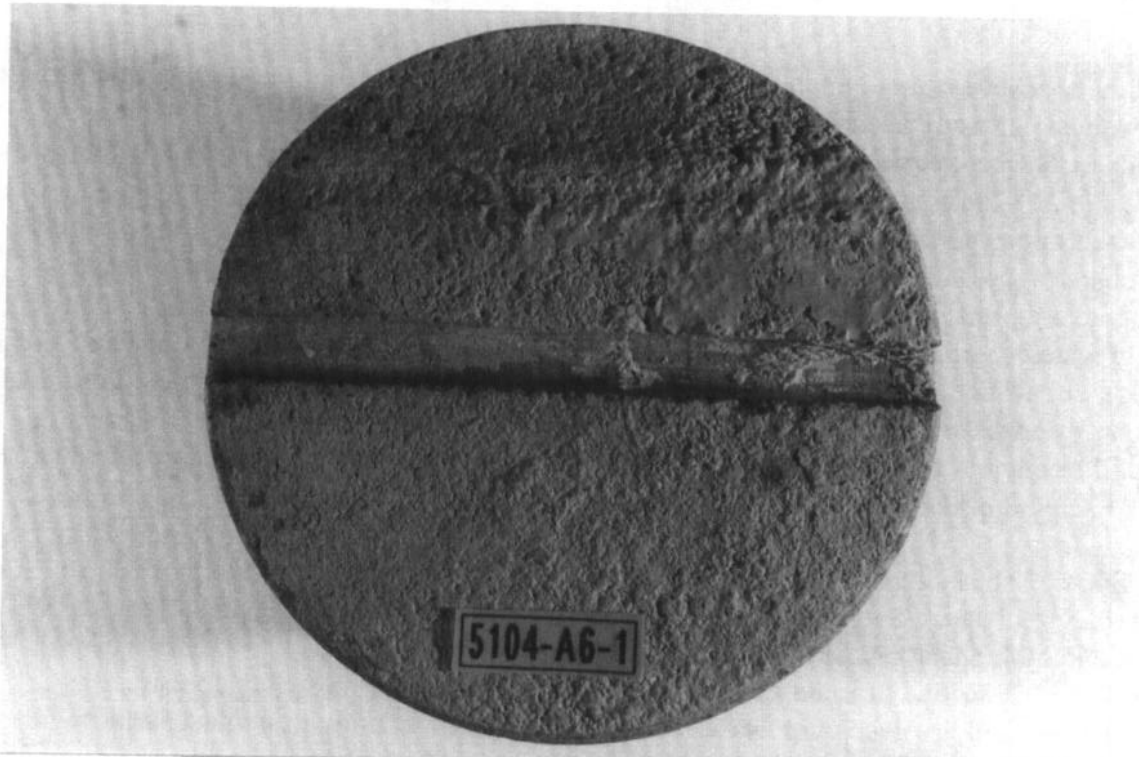


Figure 29. Core taken from Beam #6 of Abbey Road Bridge in as-received condition.

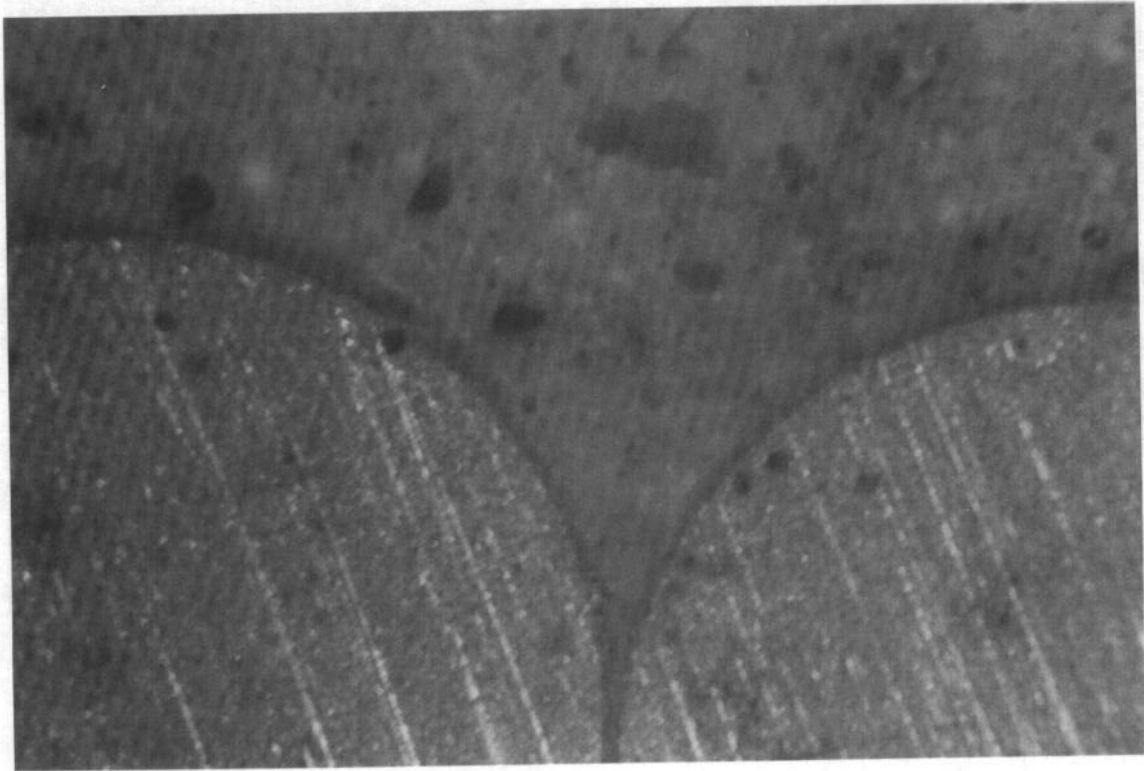
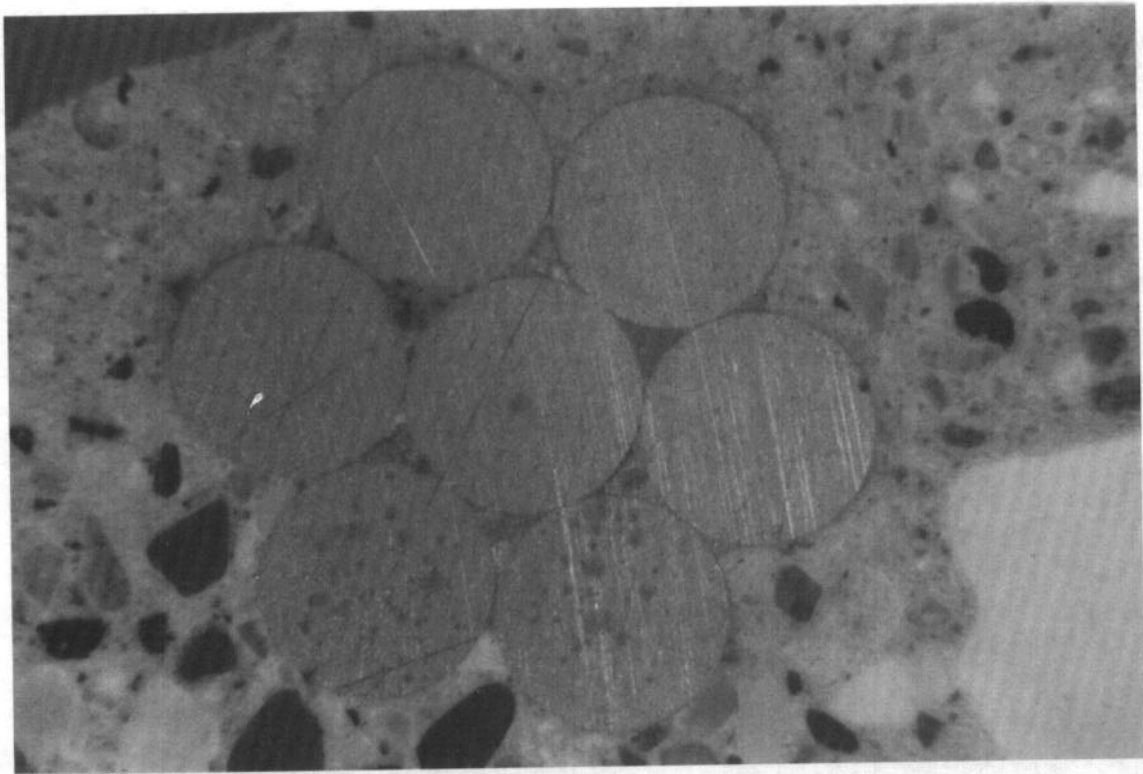


Figure 30. Section views of core taken from Beam #9 of Abbey Road Bridge.

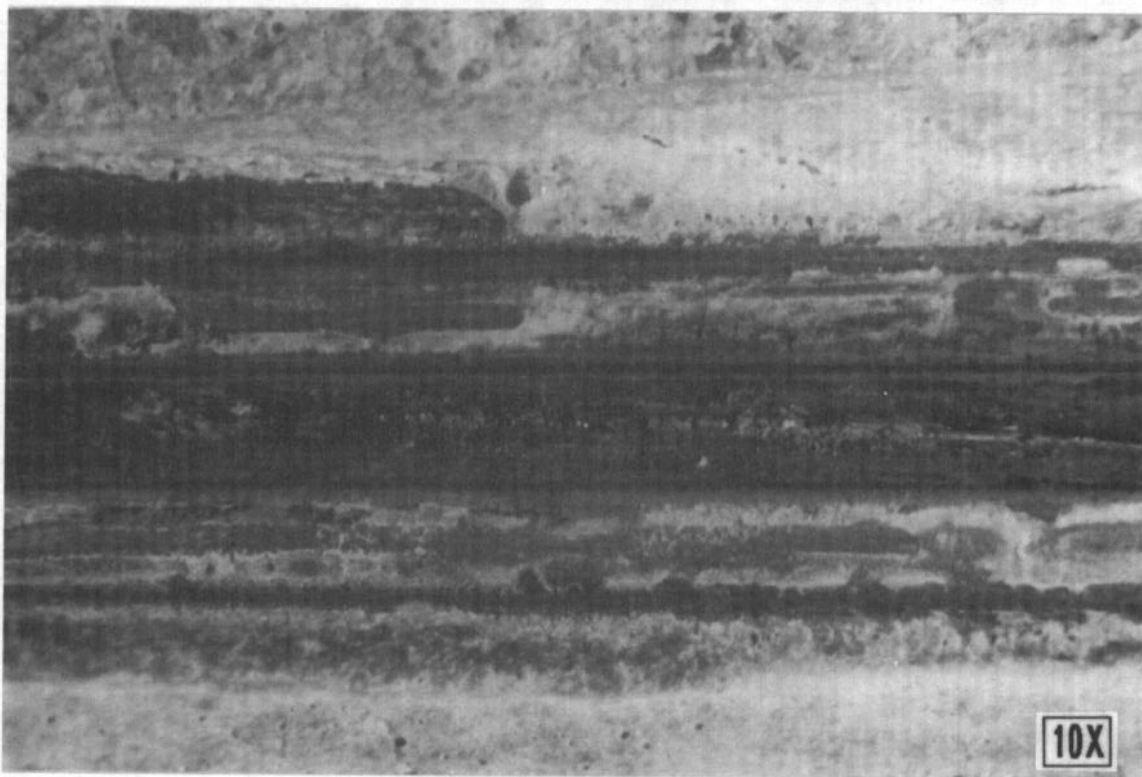
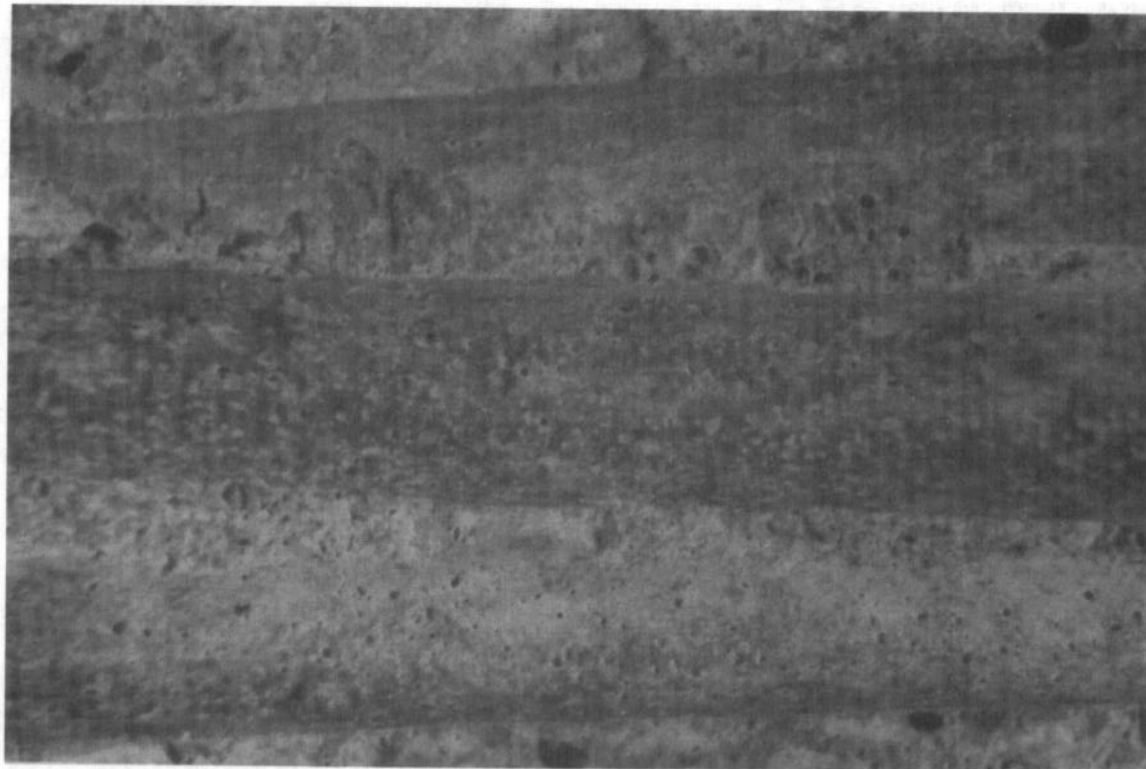


Figure 31. Optical microscope view showing fracture of core from Beam #2 of Abbey Road Bridge.

Remnants of cement paste were adhered to all of the prestressing steel wires attesting to a continuity of the physical bond between the steel and concrete following the cathodic protection treatment. The cement paste in contact with the steel was typically the normal gray color of hydrated portland cement. The paste was typically hard, dense, and compact, and occasionally showed small amounts of spherical voids in the 10- to 100- $\mu\text{m}$  size range (part of the entrained air system in the concrete). In all cores examined, intimate contact of the concrete with the prestressing steel strand has been maintained. The physical condition of the cement paste in contact with the prestressing steel strongly indicates that the CP treatment has had no adverse effect on the integrity of the paste that would result in a compromise of the bond between the cement paste and the steel. There is no difference between the different specimens in this regard.

In the optical microscopy work, comparisons were made in the color, texture, and hardness of the cement paste phase in contact with the steel and compared with similar features in the cement paste phase of concrete at sites away from the reinforcing steel. These comparisons showed virtually identical features for the two locations, strongly suggesting that the CP treatment had no adverse effect on the physical condition of the cement paste in contact with the steel. Further evidence supporting this view was established in the SEM examinations, which showed similar physical properties in cement paste examined from the two locations. The similarity in microstructure is also taken as evidence that the CP treatment has had no adverse effect on the physical integrity of the hydrated portland cement phase in contact with the prestressing steel.

The pH of the concrete defining the prestressing steel/concrete interface surface was measured immediately after revealing the surface (both sawcut and fracture surfaces). In all cases, the concrete surface in contact with the steel showed no carbonation, and had a pH in the expected range of 12 to 13.

The EDS examination of the steel/concrete bond surfaces revealed a clean layer of uniform gray colored, dense, compact, hydrated portland cement showing very low relief on the surface in contact with the steel. An example of this condition is shown in figure 32. Also shown in figure 32 is the EDS spectrum for this surface in contact with the prestressing steel. This spectrum, taken on the core from Beam #2, represents the "normal" expected phases for hydrated portland cement, and is typical of all of the specimens removed from the Abbey Road Bridge.

The EDS examination also revealed that no increase in the levels of alkali cations (Na, K) was seen on the concrete/steel interface surfaces in samples from Beams #5, #6, and #9. A slight elevated level of potassium and the appearance of sodium was observed on the interface surface of the sample from Beam #5. Confirming previous experience, the EDS analyses of the Abbey Road Bridge cores show that the application of CP current did provide a reduction in the chloride ion content at the embedded steel surface. There was a slight, but measurable decrease over distances of 5 to 50 mm (0.2 to 2.0 in) from the surface.

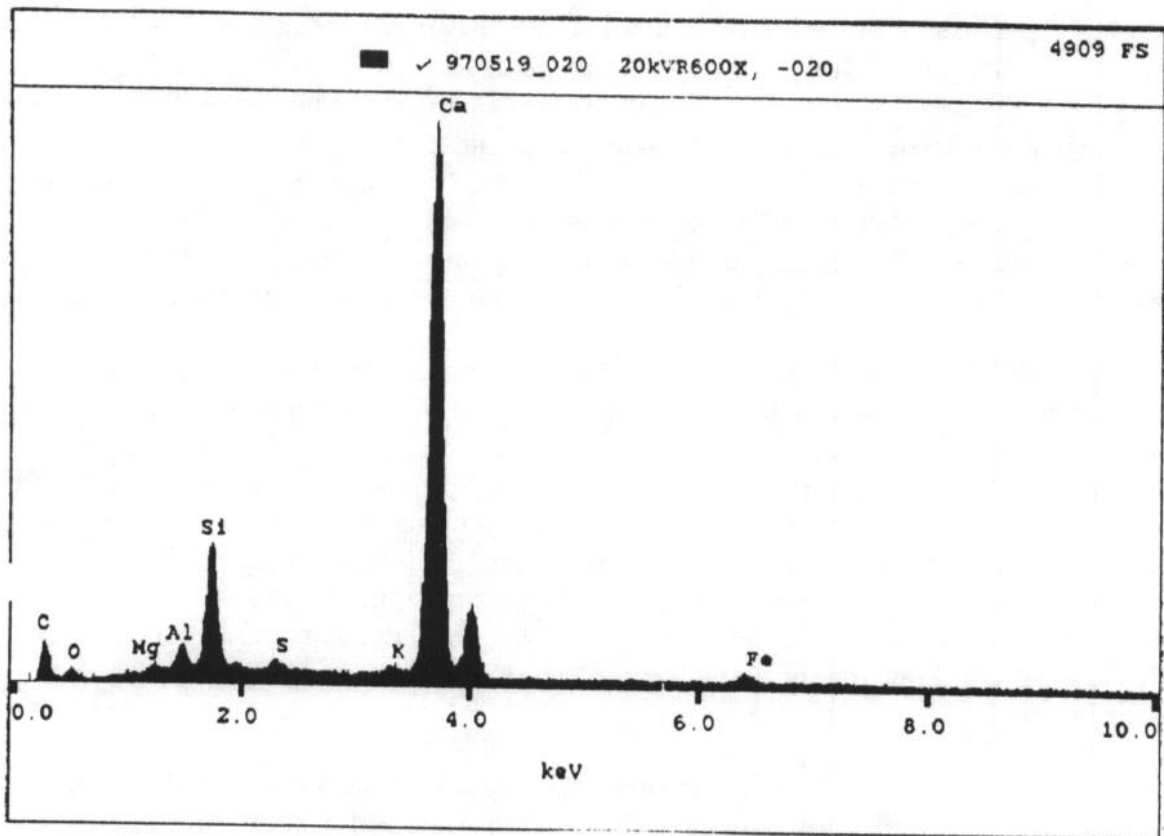


Figure 32. EDS spectrum and photograph (600X) of the steel/concrete interface in specimen from Beam #2.

The most significant observations and conclusions derived from the examination of specimens taken from the Abbey Road Bridge, as related to the effects of the CP treatment on concrete and bond quality, are as follows:

1. The CP treatment had no adverse effect on the structural integrity of the concrete contacting or adjacent to the prestressing steel.
2. The CP treatment produced no alteration in the chemistry or mineralogy of the concrete in contact with the prestressing steel.
3. Conclusions 1 and 2, along with direct observations of the physical integrity of the prestressing steel/concrete bond in all of the Abbey Road Bridge samples leads to the conclusion that the CP treatment used in this trial did not have an adverse effect on the quality of the bond between the prestressing steel and the concrete.
4. Beyond the issue of bond quality, all of the prestressing wires in the Abbey Road Bridge samples following CP treatment are judged to be in excellent condition showing virtually no loss of steel section.
5. Light surface rusting was observed on the steel surfaces on the interior of the 7-wire strands. The majority of the interstitial space between adjacent wires was filled with lubricant. The presence of this lubricant prevented the intrusion of cement paste into these spaces (which may have eliminated or minimized this corrosion).

#### Howard Frankland Bridge

None of the post-CP treatment samples provided to Lankard Materials Laboratory contained any prestressing steel. This occurred because the 50-mm- (2-in-) diameter cores were too small to restrain the stressed steel tendons.

The Howard Frankland Bridge samples were examined using the same procedures described previously for the Abbey Road Bridge samples. The principal modes of examination used optical microscopy and SEM/EDS procedures. Optical microscope views of the prestressing steel/concrete bond surfaces are shown in figure 33.



Figure 33. Optical microscope views of the Howard Frankland Bridge samples.

The concrete represented in the samples from the Howard Frankland Bridge was a non-air-entrained portland cement concrete containing a crushed limestone coarse aggregate and a natural sand. The concrete was well consolidated in all of the samples showing no abnormal amounts of gross porosity and no honeycomb. The cementitious phase in the concrete was compromised solely of well hydrated portland cement. The water-cement ratio (w/c) was estimated to fall within the range of 0.32 to 0.34. In all of the samples, the cementitious phase was medium dark gray in color, and was dense, compact, and quite hard. The coarse aggregate was a 25-mm- (1-in-) nominal maximum size biomicritic limestone, which was dominated by white subgranular particles with a high rate of water absorption. The fine aggregate was a pure quartz sand. The concrete was not air-entrained, and the total entrapped air was estimated at 1 to 2 percent.

The interface surfaces in these samples were composed principally of portland cement paste that was medium gray in color, hard, dense, and smooth. The cement paste showed occasional small streaks of iron staining, as shown in figure 34.

The water-cement ratio of the cement paste contacting the prestressing steel was comparable to that in concrete away from the prestressing steel. The hardness of the cement paste in both regions was similar, indicating that the physical integrity of the cement paste contacting the prestressing steel has not been compromised by the cathodic protection treatment. SEM photographs showed that the cement paste at the interface surfaces was dense and compact, and showed only minor amounts of submicron-size porosity.

Polished surfaces of concrete section perpendicular to the long axis of the prestressing steel were examined in the SEM, permitting a comparison of the physical features of cement paste in contact with the steel and well removed from the steel. This comparison established that, from the point of view of texture, hardness, and microstructure, the cement paste on the interface surface was comparable in all respects to cement paste in other portions of the concrete sample not in contact with the steel. The cement paste was dense and compact and showed small amounts of porosity under 10  $\mu\text{m}$  in size.

A typical EDS spectrum for the interface surfaces in the Howard Frankland Bridge samples is shown in figure 35. Iron (Fe) levels were slightly higher than "normal" reflecting the iron staining shown previously in figure 34. Alkalies (Na, K) were commonly, although not always, present. The alkali content of the paste in the carbonated areas was typically slightly higher than in uncarbonated areas reflecting, perhaps, on the accessibility of pore water to those areas.

About one-half of the interface areas examined showed trace levels of chloride. The chlorides tended to be concentrated near areas of porosity in the interface surface cement paste, again reflecting the condition of pore water accessibility. There are indications that the CP treatment transported some of the chloride away from the steel-concrete interface surface.

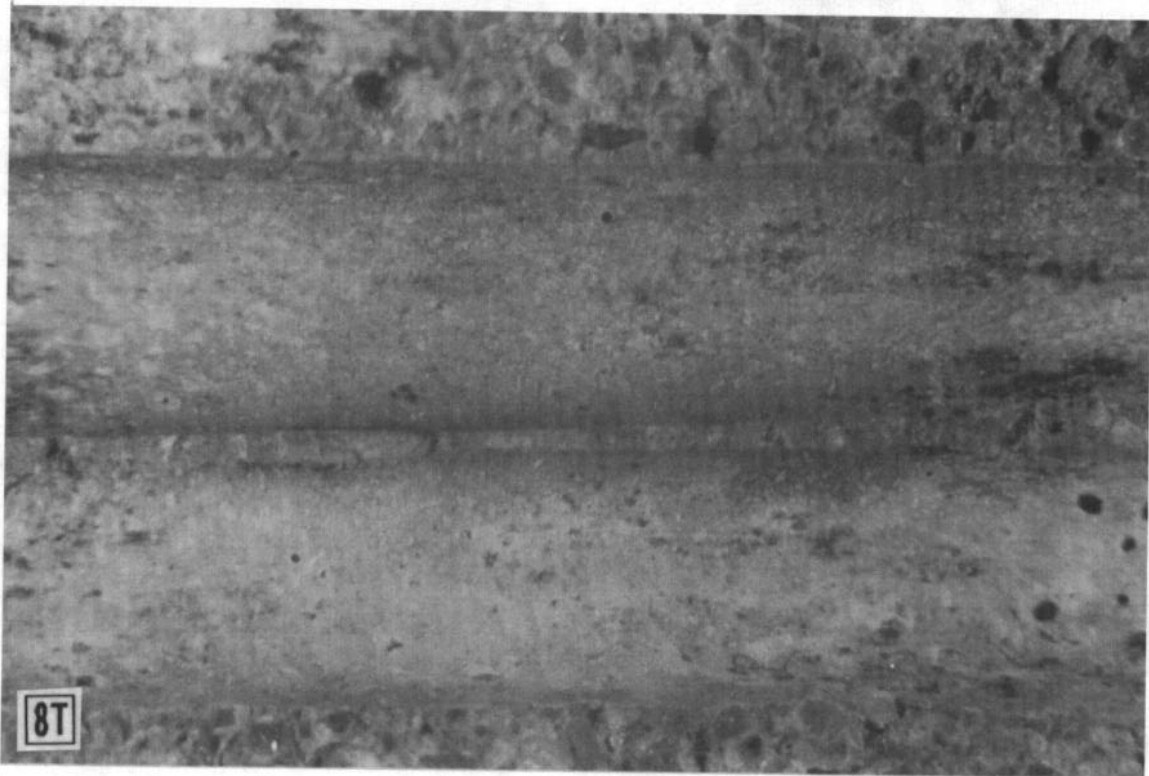
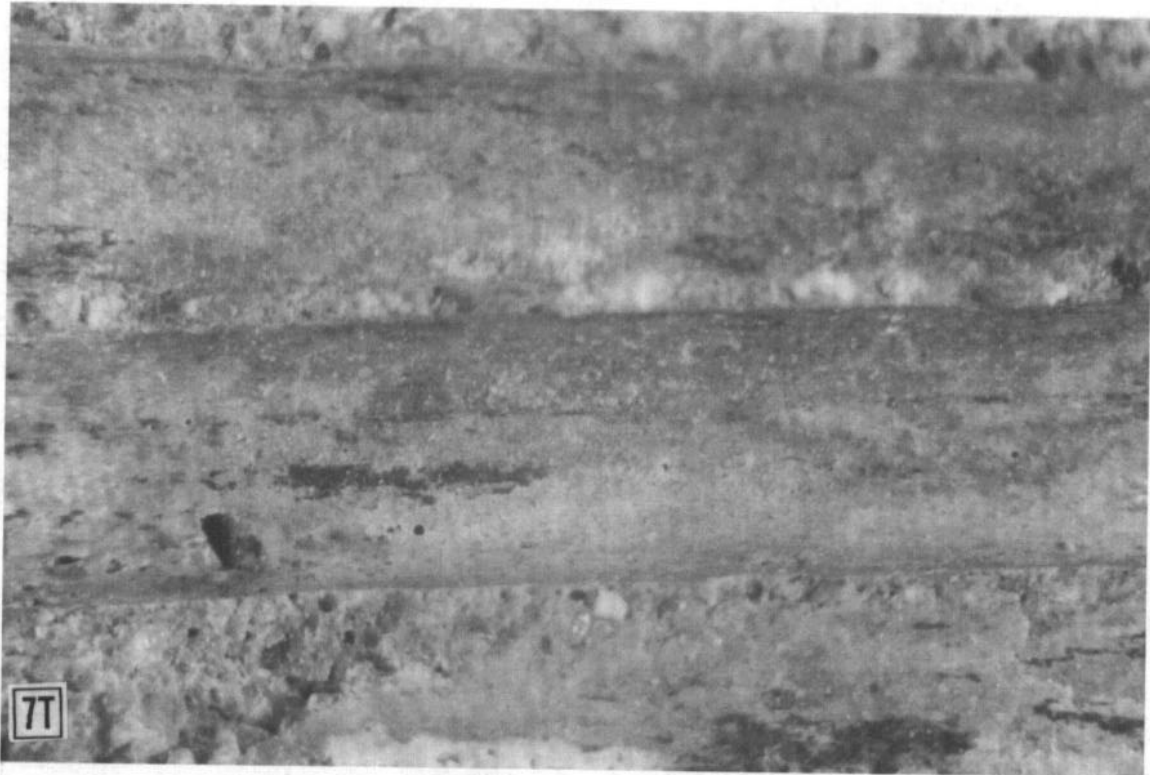


Figure 34. Prestressing steel/concrete interface surfaces in Howard Frankland Bridge samples.

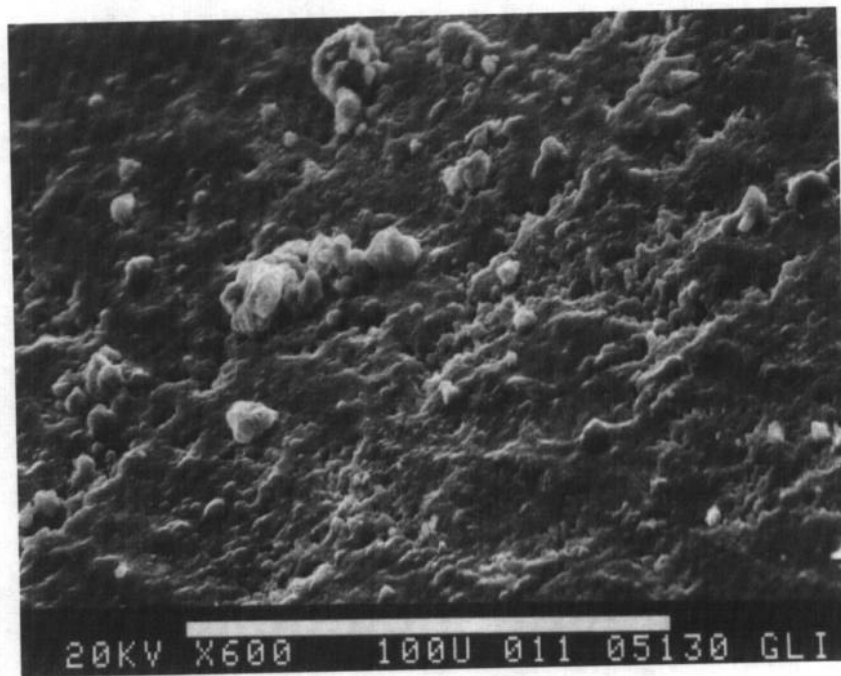
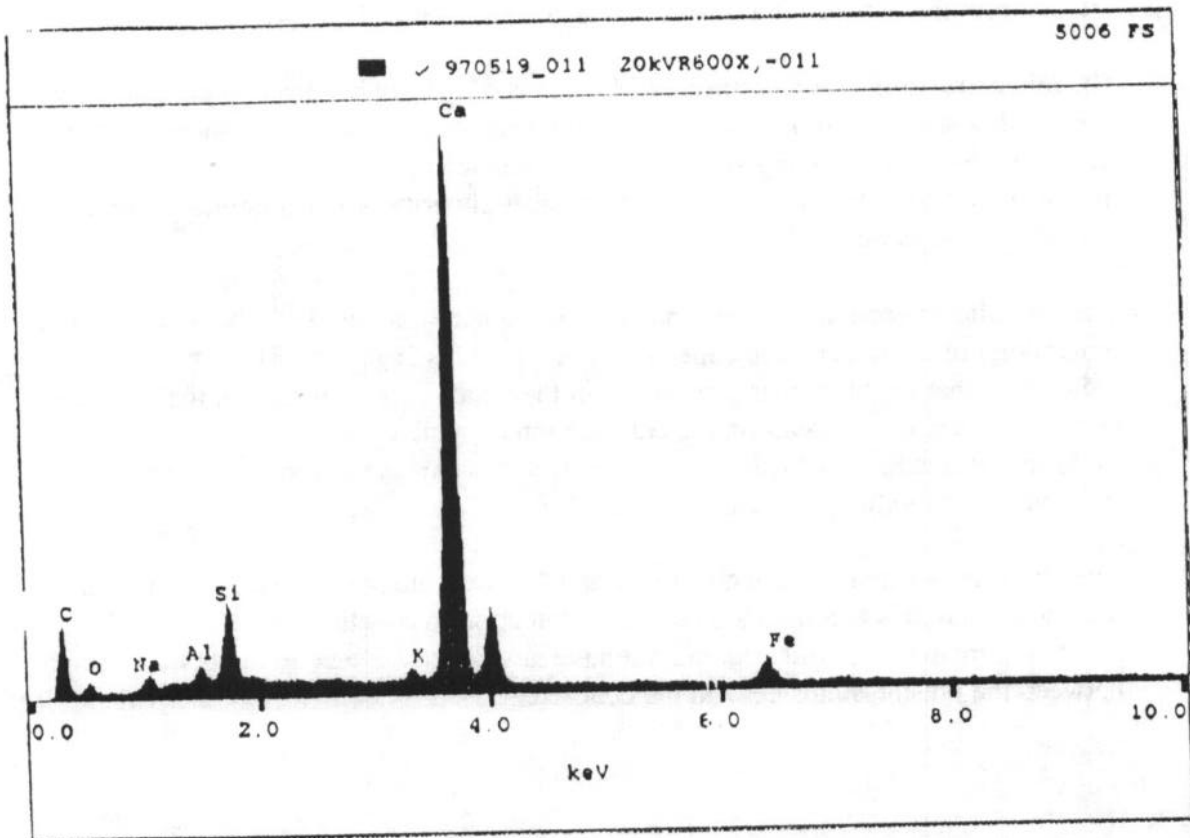


Figure 35. EDS spectrum and photograph (600X) of the prestressing steel/concrete interface surface in Howard Frankland Bridge sample.

The most significant observations and conclusions derived from the examination of the specimens taken from the Howard Frankland Bridge are summarized below.

1. The microstructure, color, texture, and hardness of the cement paste in contact with the prestressing steel is comparable to that of the cement paste phase in concrete not in contact with the prestressing steel. There are no indications that the cathodic protection treatment had any adverse effect on the physical integrity of the concrete in contact with the prestressing steel.
2. The cathodic protection treatment had no significant effect on the bulk chemistry or mineralogy of the concrete in contact with the prestressing steel. There were indications that slight increases occurred in the alkali-bearing phases at the interface surface and a slight decrease in the chloride ion content at the interface surface. Both of these features have previously been identified as expected events in concrete subjected to cathodic protection current.
3. The observations made in conclusions 1 and 2 above, along with other findings and observations in this examination can be drawn upon to conclude that the cathodic protection treatment in this trial did not have any adverse effect on the bond strength between the prestressing steel and the concrete.

## CHAPTER 6. CONCLUSIONS AND RECOMMENDATIONS

1. Based on cathodic protection (CP) field trials on three marine and nonmarine bridges, it is concluded that CP can be effectively used to control the corrosion of prestressing steel in pretensioned bridge members with careful monitoring of applied current and voltage.
2. For structures with very nonhomogeneous concrete resistance, it may be difficult to achieve cathodic protection criteria at sites where resistivity is high, while at the same time precluding hydrogen generation at sites where resistance is low. This was evident during operation of CP zones utilizing metallized zinc anodes on prestressed box beams of the Abbey Road Bridge, conductive rubber anodes on prestressed pilings of the Howard Frankland Bridge, and to a lesser extent, conductive paint anodes on prestressed box beams of the West 130<sup>th</sup> Street Bridge. Diverse concrete resistance is most often caused by a difference in moisture content, but may also be influenced by other factors, such as depth-of-cover, chloride content, anode contact resistance, and distance from anode power feed. This concern is most relevant where surface-applied anodes are used.
3. Operation of CP systems installed on structures that contain prestressed steel is best accomplished in constant voltage mode. The operating voltage should be selected in a manner so that potentials required to generate hydrogen will not be attained at the prestressed steel surface. The same objective can be accomplished by operating in constant current mode while limiting the rectifier voltage, provided that the same strategy is used in selection of the rectifier voltage. This was demonstrated by operating the CP system utilizing titanium mesh anodes in fiberglass jackets on pilings of the Howard Frankland Bridge.
4. Cathodic protection treatments of 32 and 37 months (charges of 48.6 and 87.5 A-h/m<sup>2</sup>) had no adverse effect on the structural integrity of the concrete contacting or adjacent to the steel, and produced no alteration in the chemistry or mineralogy of the concrete in contact with the prestressing steel. These conclusions, together with direct observation of the physical integrity of the prestressing steel/concrete bond, led to the conclusion that the CP treatments had no adverse effect on the quality of bond between the prestressing steel and the concrete.
5. Although a small amount of hydrogen was indicated for some of the post-CP prestressed steel specimens analyzed, this finding cannot be correlated with any measured mechanical property or data acquired during operation, and is therefore not considered significant.
6. The ductility of all post-CP prestressed steel specimens was relatively high, and is consistent with little or no embrittlement having occurred, despite the selection of some specimens from sites where steel potentials were frequently very negative (< -900 mV versus SCE).

7. Utilization of anodes in direct contact with seawater resulted in excessive leakage of current to submerged portions of the structure. Although this aspect does not preclude adequate protection of the steel from corrosion, it makes testing of CP criteria by normal techniques difficult or impossible, and may lead to very negative steel potentials where concrete is saturated.
8. The Devanathan-type hydrogen probe used in this contract was not a reliable indicator of hydrogen evolution. Probes frequently showed a response at potentials far too positive to permit hydrogen evolution, and at other times failed to indicate a response when potentials were very negative.
9. Confirming previous experience, analyses of post-CP specimens showed that the application of cathodic protection current did provide a reduction in chloride ion concentration at the embedded steel surface.
10. The bond of conductive paint to the concrete surface at the West 130<sup>th</sup> Street Bridge was compromised by either unacceptable moisture content or excessive current during early operation, or both. Conductive paint appears to be more sensitive in this regard than other anodes tested.

## REFERENCES

1. Pourbaix, Marcel, *Atlas of Electrochemical Equilibria in Aqueous Solutions*, National Association of Corrosion Engineering, Houston, 1974.
2. Wagner, J., et al., *Cathodic Protection Developments for Prestressed Concrete Components*, Publication No. FHWA-RD-92-056, March 1993.
3. Hartt, W.H., "Cathodic Protection and Environment Cracking of Prestressing Steel," NACE Corrosion 89, Paper 382, New Orleans.
4. Hope, B.B. and J.S. Poland, "Cathodic Protection and Hydrogen Generation," *ACI Materials Journal*, Sept.-Oct. 1990, p. 469.
5. Hartt, W.H., C.C. Kumria, and R.J. Kessler, "Influence of Potential, Chlorides, pH, and Precharging Time on Embrittlement of Cathodically Polarized Prestressed Steel," *Corrosion*, Vol. 49, 1993, p. 377.
6. Bartholomew, J.J., et al., "Control Criteria and Materials Performance Studies for Cathodic Protection of Reinforced Concrete," ELTECH Research Corporation, National Research Council Report No. SHRP-S-670, 1993.
7. Hartt, W.H., "A Critical Evaluation of Cathodic Protection for Prestressed Steel in Concrete," in *Corrosion of Reinforcement in Concrete*, eds., C.L. Page, K.W.J. Treadway, and P.B. Bamforth (London, UK: Elsevier, *Appl. Sci.*, 1990), p. 515.
8. Hartt, W.H., Joubert, E., and Kliszowski, S., *Long Term Effects of Cathodic Protection on Prestressed Bridge Components*, Publication No. FHWA-RD-96-029, 1996.
9. Stauder, A.L. and Hartt, W.H., "Brittle Fracture Propensity and Cathodic Protection Qualification of Damaged Pretensioned Tendons in Concrete," to be presented at NACE Corrosion 98, Paper 635, San Diego, March 22-27, 1998.
10. Enos, D.G., Williams, A.J., Clemena, G.G., and Scully, J.R., "Impressed Current Cathodic Protection of Steel Reinforced Concrete Pilings: Protection Criteria and the Threshold for Hydrogen Embrittlement," NACE Corrosion 97, Paper 241, New Orleans, March 10-14, 1997.
11. Stratfull, R.F., E.C. Noel, and K. Seyoum, *Evaluation of Cathodic Protection Criteria for the Rehabilitation of Bridge Decks*, Publication No. FHWA-RD-83-048, November 1983.
12. Schell, H.C. and D.G. Manning, "Evaluating the Performance of Cathodic Protection Systems on Reinforced Concrete Bridge Substructures," *Materials Performance*, NACE, July 1985, pp. 18-25.

13. Bazzoni, B. and L. Lazzari, "A New Approach for Automatic Control and Monitoring of Cathodically Protected Reinforced Concrete Structures," NACE Corrosion 92, Paper 196, Nashville, April 27-30, 1992.
14. Bullard, S.J., Covino, B.S., Holcomb, G.R., Cramer, S.D., and McGill, G.E., "Bond Strength of Thermally-Sprayed Zinc on Concrete During Early Electrochemical Aging," NACE Corrosion 97, Paper 232, New Orleans, March 10-14, 1997.
15. Lankard, D.R., N.J. Scaglione, and J.E. Bennett, "Petrographic Examination of Reinforced Concrete from Cathodically Protected Structures," in *Petrography of Cementitious Materials*, ASTM STP-1215, eds., S.M. DeHayes and D. Stark, American Society for Testing and Materials, Philadelphia, 1994.
16. American Society for Testing and Materials, Volume 04.02, Concrete and Aggregates Specification ASTM C 856-83, "The Standard Practice for Petrographic Examination of Hardened Concrete."